Spectrochimica Acta Part A: Molecular and Biomolecular Spectroscopy 137 (2015) 1315–1333

Contents lists available at ScienceDirect

Spectrochimica Acta Part A: Molecular and Biomolecular Spectroscopy

journal homepage: www.elsevier.com/locate/saa

FT-IR, FT-Raman, NMR and UV–Vis spectra and DFT calculations of 5-bromo-2-ethoxyphenylboronic acid (monomer and dimer structures)

E.B. Sas [a], E. Kose [b], M. Kurt [a,*], M. Karabacak [c]

[a] Department of Physics, Ahi Evran University, Kırsehir, Turkey
[b] Department of Physics, Celal Bayar University, Manisa, Turkey
[c] Department of Mechatronics Engineering, H.F.T. Technology Faculty, Celal Bayar University, Turgutlu, Manisa, Turkey

HIGHLIGHTS

- Monomeric conformations and dimeric structure of 5-bromo-2-ethoxyphenylboronic acid were investigated.
- The compound was characterized by FT-IR, FT-Raman, NMR and UV spectroscopies.
- The vibrational frequencies, chemical shifts and electronic absorption wavelengths were calculated by DFT method.

GRAPHICAL ABSTRACT

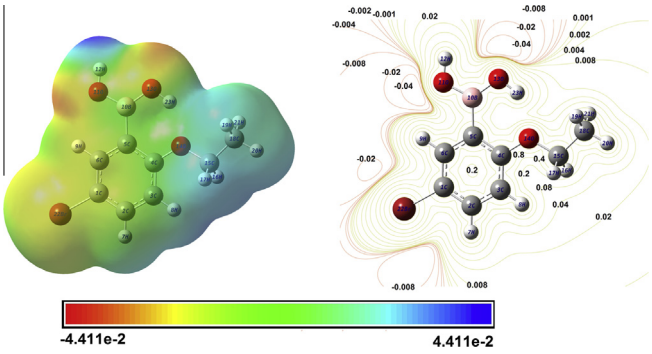

ARTICLE INFO

Article history:
Received 12 May 2014
Received in revised form 19 August 2014
Accepted 24 August 2014
Available online 2 September 2014

Keywords:
5-Bromo-2-ethoxyphenylboronic acid
FT-IR and FT-Raman spectra
NMR and UV spectra
NBO and NLO
DFT

ABSTRACT

In this study, the Fourier Transform Infrared (FT-IR) and Fourier Transform Raman (FT-Raman) spectra of 5-bromo-2-ethoxyphenylboronic acid (5Br2EPBA) are recorded in the solid phase in the region 4000–400 cm^{-1} and 3500–10 cm^{-1}, respectively. The ^{1}H, ^{13}C and DEPT nuclear magnetic resonance (NMR) spectra are recorded in DMSO solution. The UV–Vis absorption spectrum of 5Br2EPBA is saved in the range of 200–400 nm in ethanol and water. The following theoretical calculations for monomeric and dimeric structures are supported by experimental results. The molecular geometry and vibrational frequencies in the ground state are calculated by using DFT methods with 6-31G(d,p) and 6-311G(d,p) basis sets. There are four conformers for the present molecule. The computational results diagnose the most stable conformer of 5Br2EPBA as *Trans–Cis* (TC) form. The complete assignments are performed on the basis of the total energy distribution (TED) of vibrational modes, calculated with scaled quantum mechanics (SQM) method in parallel quantum solutions (PQS) program. The ^{1}H and ^{13}C NMR chemical shifts of 5Br2EPBA molecule are calculated by using the Gauge Invariant Atomic Orbital (GIAO) method in DMSO and gas phase for monomer and dimer structures of the most stable conformer. Moreover, electronic properties, such as the HOMO and LUMO energies (by TD-DFT and CIS methods) and molecular electrostatic potential surface (MEPs) are investigated. Stability of the molecule arising from hyper-conjugative interactions, charge delocalization is analyzed using natural bond orbital (NBO) analysis. Nonlinear optical (NLO) properties and thermodynamic features are presented. All calculated results are compared with the experimental data of the title molecule. The correlation of theoretical and experimental results provides a detailed description of the structural and physicochemical properties of the title molecule.

* Corresponding author. Tel.: +90 386 211 45 54; fax: +90 386 252 80 54.
E-mail address: kurt@gazi.edu.tr (M. Kurt).

http://dx.doi.org/10.1016/j.saa.2014.08.049
1386-1425/

Introduction

Interest in compounds containing boronic acid functionality is increasing rapidly. This interest stems from the use of boronic acids as pharmaceutical agents [1] and their utilization in the synthesis of other boron derivatives that exert a variety of physiological activities [2,3]. A variety of boron compounds can be used as cross linkers in the hydrogel developed for the treatment of lung volume reduction. Crosslinker is selected from the group consisting of boric acid, borates, boronic acids, boronates and boroxines. Besides, crosslinker is derived from an optionally-substituted phenyl boronic acid, an optionally-substituted phenyl boronate, or an optionally-substituted phenyl boroxine.

5-Bromo-2-ethoxyphenylboronic acid is used as crosslinkers in the hydrogel may be used to treat any form of abnormal cellular growth (e.g., tumors, cancer, etc.) by targeting a non-toxic, yet therapeutically effective, polycationic composition to an area of diseased tissue (e.g., a tumor, adenoma, cancer, precancer, or other abnormal lesion). A vast number of therapeutic agents may be incorporated in the hydrogel. In general, therapeutic agents which may be incorporated include, without limitation: anti-infective such as antibiotics and antiviral agents; anorexics; anticonvulsants; antidepressants; antidiuretics agents; anti-histamines; anti-inflammatory agents; anti-migraine preparations; anti parkinsonism drugs; central nervous system stimulants [4]. The wide types of derivatives of boronic acids are separated many areas from supra-molecular and analytical chemistry (material science, medicine, biology, catalysis) to crystal engineering. They are used as reagents with in organic synthesis, enzyme inhibitors, catalysts, protecting groups, and affinity purification agents, receptors for saccharide sensing, neutron capturing agents for cancer therapy, bio conjugates, and protein labels [5]. Identify carbohydrates that are potentially suitable linear linkers—in both a geometrical and a chemical sense—for linear and higher dimensional boronic acid nodes were reported [5]. A novel class of bacterial mutagen that may not act by direct covalent binding to DNA were published by O'Donovan et al. [6]. Biomedical applications of boronic acids derivatives were reported [7,8].

Phenylboronic acid, a phenyl substituent and two hydroxyl groups attached to boron, is the most important derivatives of boronic acid. The molecular structure and spectroscopic properties of phenylboronic acid and its derivatives were gained in the literature. The crystal and molecular structures of phenylboronic acid were reported by Rettig and Trotter [9]. Cyrański et al. [10] prepared the molecular structures of phenylboronic acid and its dimer by using X-ray structural analysis and spectroscopic methods. The crystal structures of 2,4-difluorophenylboronic acid were presented by Rodriguez et al. [11]. Shimpi et al. [12] reported the crystal structures of 4-chloro- and 4-bromophenylboronic acids and hydrates of 2- and 4-iodophenylboronic acid in two different forms, which were characterized by single-crystal X-ray diffraction method. Faniran and Shurvell [13] analyzed infrared spectra of phenylboronic acid and diphenyl phenylboronate. The vibrational spectra and molecular structure of the 4-chlorophenylboronic acids [14], 3-bromo- [15] and 4-bromophenylboronic acid [14], 3,4- and 3,5-dichlorophenylboronic acid [16,17], and 2,6-dimethoxy phenylboronic acid [18] were studied experimentally and theoretically. Moreover, the experimental and theoretical investigation of the conformation, vibrational and electronic transitions of 2,3- and 3,5-difluorophenylboronic acid molecules [19,20], acenaphthene-5-boronic acid [21], methylboronic acid [22] and 2-Thienylboronic acid [23] were investigated.

Literature survey showed that, there is no experimental (with combined theoretical calculations) spectroscopic study performed on the conformation, vibrational (FT-IR and FT-Raman), NMR and UV–Vis spectra about on 5Br2EPBA. To overcome this deficiency, we aim to represent the detailed spectroscopic studies of 5Br2EPBA by FT-IR and FT-Raman, ^{1}H, ^{13}C, DEPT 135 NMR and UV–Vis spectral techniques experimentally and theoretically. We supported to these analyses with the thermodynamical and NLO properties, NBO analysis, and density of states, MEPs features of the 5Br2EPBA molecule. Also, thermodynamical properties for example heat capacity, entropy and enthalpy change at increasing temperatures were calculated to have more characteristics of the studied molecule. Meticulous notes were prepared on the effect of intermolecular O–H···O hydrogen bonding, modeled at the DFT/B3LYP level, on the bond distances and angles, calculated frequencies and chemical shifts of the title molecule.

Experimental

The 5Br2EPBA molecule is provided from Across Organics Company in solid state with a stated purity of 97% and it was used as no extra purification. The title molecule is processed by the experimental (FT-IR, FT-Raman, NMR and UV–Vis) techniques. The FT-IR spectrum of the studied molecule is recorded in the region 4000–400 cm^{-1} on a Perkin Elmer FT-IR System Spectrum BX spectrometer calibrated using polystyrene bands. The sample is prepared using a KBr disc technique because of the solid state. The spectrum is recorded with a scanning speed of 10 cm^{-1} min^{-1} and the spectral resolution of 4.0 cm^{-1}. FT-Raman spectrum is recorded using 1064 nm line of Nd:YAG laser as excitation wavelength in the range of 4000–50 cm^{-1} on a Bruker RFS 100/S FT-Raman. The detector is a liquid nitrogen cooled Ge detector. Five hundred scans were accumulated at 4 cm^{-1} resolution using a laser power of 100 mW. The ^{1}H, ^{13}C and DEPT 135 NMR spectra are carried out in DMSO solution on a Brucker DPX 600 MHz spectrometer using tetramethylsilane (TMS) as an internal reference at 25 °C. The UV absorption spectrum is registered in ethanol and water on Shimadzu UV-1800 PC spectrophotometer in the spectral region 200–400 nm.

Computational details

The geometrical parameters, IR, Raman, (^{1}H and ^{13}C) NMR and UV–Vis spectra of the studied molecule were calculated by dint of Gaussian09 suite of quantum chemical codes [24]. Due to accepted as a cost-effective approach and to understand of theoretical calculations of organic molecules, the density functional theory (DFT) [25] with the Becke's three-parameter hybrid functional (B3) [26], for the exchange part and the Lee–Yang–Parr (LYP) correlation function [27] are utilized for the computation of molecular structure, vibrational frequencies and energies of optimized structures.

To find the most stable structure of the present molecule within four possible conformers are proposed as named *Trans–Cis* (TC), *Cis–Cis* (CC), *Trans–Trans* (TT), and *Cis–Trans* (CT). They are optimized by using by B3LYP with the 6-31G(d) and 6-311G(d,p) basis sets for all proposed conformers. Unavailability of the crystal structure of the present molecule, potential energy scan was performed to get the most stable geometry of the studied molecule using B3LYP/6-311G(d,p) level of theory. The computational results are showed that the most stable conformer of 5Br2EPBA is TC form. The optimized structural parameters are used in the vibrational frequencies, isotropic chemical shifts and electronic properties for monomeric and dimeric structures. The scale factors are used to obtain the best agreement results with the experimental data. The global scaling factor of 0.9603 and 0.9610 are selected for B3LYP/6-31G(d) and B3LYP/6-311G(d,p), respectively. The Raman activities (S_{Ra}) converted to relative Raman intensities (I_{Ra}) are derived from the intensity theory of Raman scattering [5,6]. The

theoretical results have enabled us to make the detailed assignments of the experimental IR and Raman spectra of the title molecule. The TED of fundamental vibrational modes is calculated by using the SQM method and PQS program [28,29]. The ^{1}H and ^{13}C NMR are performed GIAO method [30,31] by using the optimized parameters obtained with 6-31G(d) and 6-311G(d,p) basis sets, in DMSO solution and gas phase. Due to GIAO method is one of the most common approaches for calculating nuclear magnetic shielding tensors. UV–Vis spectrum, electronic transitions, vertical excitation energies, absorbance and oscillator strengths of the headline molecule are calculated by CIS/6-311G(d,p) and TD-DFT/6-311G(d,p) levels in ethanol, water solutions and gas phase. In order to understand various second order interaction between the filled and empty orbitals, NBO calculations are made using Gaussian09 package at the DFT/B3LYP/6-311G(d,p) level. NBO analysis provides an efficient methods for studying inter- and intramolecular bonding and interaction among bonds.

GaussSum 2.2 [32] was utilized to plot density of states; the total density of states (TDOS), the partial density of states (PDOS) and overlap population density of states (OPDOS or COOP) diagrams and to have analysis group contributions of molecular orbitals. The PDOS and OPDOS graphs were performed by convoluting the molecular orbital information with Gaussian curves of unit height and a FWHM (Full Width at Half Maximum) of 0.3 eV. The statistical thermodynamic functions (the heat capacity, entropy, and enthalpy), MEPs and NLO properties of 5Br2EPBA molecule were obtained by using B3LYP/6-311G(d,p) method.

Results and discussion

The title molecule 5Br2EPBA has C_6H_3 group, Br (Bromine) atom, CH_3CH_2O- (ethoxy), and $B(OH)_2$ group. The possible structures of the title molecule are investigated, due to model system $B(OH)_2$ and the positions of the hydrogen atoms, whether directed away from or toward the ring. This model offered four conformers/isomers as named TC, CC, CT, and TT are given in Fig. 1.

Energetics and potential energy surface (PES) scan

The energies of proposed (based on the location of hydrogen atom) different conformations of the present molecule are optimized DFT/B3LYP with the 6-31G(d) and 6-311G(d,p) basis sets for C_1 and C_s point group symmetries. The calculations are showed that TC form is the more stable conformer than the other conformers. There is no negative frequency in the conformers TC and TT, while CT and CC forms of the molecule have the negative frequency (imaginary frequency) for C_s group symmetry. Because of this reason and the based on the energy; the as reference point [the lowest energy (C_s group symmetry of TC)], the relative energy of the other conformers was as: $\Delta E = E(C_n) - E(C_{TC})$. The energies and energy differences of the title molecule are described in Table 1. The TC conformer has energy differing from by value 4.6177–9.1799 kcal/mol (from 4.5399 to 9.1552 kcal/mol for C_1 symmetry point group) than the other conformers of the studied molecule for C_s symmetry point group. The TC form of the molecule is the most stable therefore, the discussions especially refer for TC form (C_s symmetry).

To describe conformational properties of 5Br2EPBA, a conformation analysis is performed between phenyl ring and $B(OH)_2$ group system. To obtain the energy profile of the four (TC/CT conformer the same scan) proposed conformers as a function of T(H11–O10–C5–C6), torsion angle was varied from 0° to 360° by changing every 10° by using B3LYP/6-311G(d,p). Namely, the potential energy curve is done by using scanning $B(OH)_2$ group made over the phenyl ring. The conformational analysis of the molecule showed that there are two local minima near 0° (or

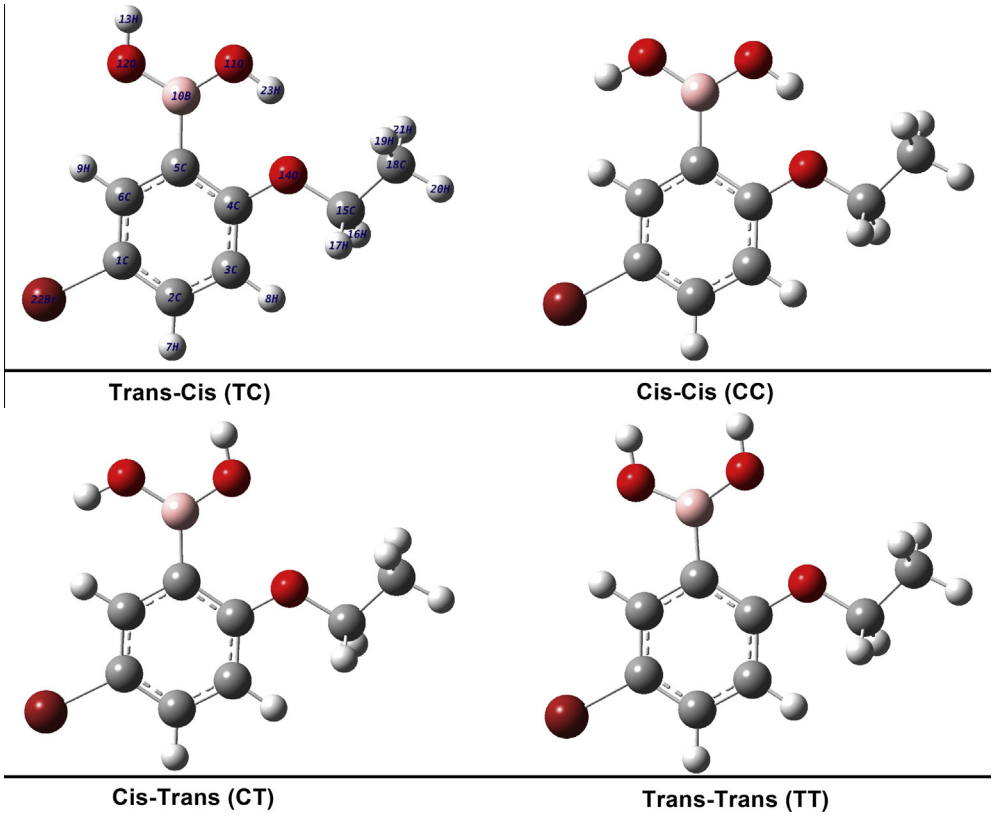

Fig. 1. The theoretical optimized geometric structures of 5Br2EPBA.

Table 1
Calculated energies and energy differences for four possible conformers of 5Br2EPBA by DFT (B3LYP/6-311G(d,p)) method.

Conformers	Energy		Energy differences[a]		Dipole moment	Imaginary frequencies
	(Hartree)	(kcal/mol)	(Hartree)	(kcal/mol)	(Debye)	(cm^{-1})
C_s group symmetry						
Trans–Cis (TC)	−3135.81842903	−1967755.8545	0.0000	0.0000	4.5102	–
Cis–Cis (CC)	−3135.81107022	−1967751.2368	0.0074	4.6177	4.7045	−37.64
Cis–Trans (CT)	−3135.80598082	−1967748.0431	0.0124	7.8114	1.9703	−69.03
Trans–Trans (TT)	−3135.80379996	−1967746.6746	0.0146	9.1799	4.0212	–
C_1 group symmetry						
Trans–Cis (TC)	−3135.81842890	−1967755.8544	0.0000	0.0001	4.5090	–
Cis–Cis (CC)	−3135.81119419	−1967751.3146	0.0072	4.5399	4.7007	–
Cis–Trans (CT)	−3135.80815582	−1967749.4080	0.0103	6.4465	2.6290	–
Trans–Trans (TT)	−3135.80383929	−1967746.6993	0.0146	9.1552	4.0184	–

[a] Energies of the other three conformers relative to the most stable TC conformer.

360°) and 140° (or 230°) for TC/CT conformers, one local minima near 0° (or 180° or 360°) for TT conformer, and one local minima near 10° (or 170° or 190° or 350°) for CC conformer based on T(H11–O10–C5–C6), torsion angles, given in Fig. S1. The conformational analysis showed that the TC conformer is the most stable for 0°/360° torsion angle of 5Br2EPBA molecule.

Geometrical structures

The crystal structure of the studied molecule is not available; therefore, the optimized structures were compared with the structurally similar molecules as following discussions. The conformers/isomers of the title molecule and atomic numbering schemes (based on TC form) are shown in Fig. 1. The dimer structure of TC conformer is shown in Fig. 2. The optimized structure parameters of the studied molecule, in accordance with the atom number in Fig. 1, (bond lengths and bond angles) for monomer and dimer structures of the TC conformer are listed in Table 2. The optimized geometry parameters four conformers of 5Br2EPBA molecule are also given in Table S1.

The C–C and C–H bond lengths of the molecule are approximately (except little difference) equal to for experimental values [9,12]. The C–C bond lengths were observed for phenylboronic acid (PBA), from 1.378 to 1.404 Å [9], these bond lengths were observed in the range of 1.365–1.393 Å (4-chloro-) and 1.365–1.392 Å (4-bromo-) [12] and calculated in the region 1.391–1.404 Å [14] for 4-chloro and 4-bromophenylboronic acid molecules. The bond lengths are calculated in the range of 1.387–1.410 Å for 2-fluorophenylboronic acid [33] and from 1.384 to 1.407 Å for 2,3-difluorophenylboronic acid [19] by using DFT method. In this study, the C–C bond lengths are calculated (for monomer structure of TC conformer) between 1.388 and 1.411 Å by using B3LYP/6-311G(d,p) and 1.390 and 1.413 Å by using B3LYP/6-31G(d) methods, showing good correlation for derivatives of boronic acids [9,12,14,19,33]. However there is seen increasing for bond length of C4–C5, this can be the effect of attached substituent these atoms. The dimer structure showed the same results with the monomer ones. The C–H bond lengths can be divided into four groups: ring, boron, methyl and ethyl groups. These values are bigger than 1 Å.

The bond lengths of B–O were observed at 1.362 Å and 1.378 Å for phenylboronic acid [9], and at 1.359 Å and 1.372 Å for 4-bromophenylboronic acid molecule [12]. The prior work, the B–O bond lengths including for different forms were calculated at 1.366 Å and 1.373 Å for 3,4-dichlorophenylboronic acid [16]. The B–O bond lengths were also obtained ca. 1.360 Å and 1.375 Å in previous study [19]. In this study, the optimized B–O bond lengths (B_{10}–O_{13} and B_{10}–O_{11}) are calculated at 1.366,1.370 Å and 1.363,1.367 Å by 6-31G(d) and 6-311G(d,p) basis sets, respectively.

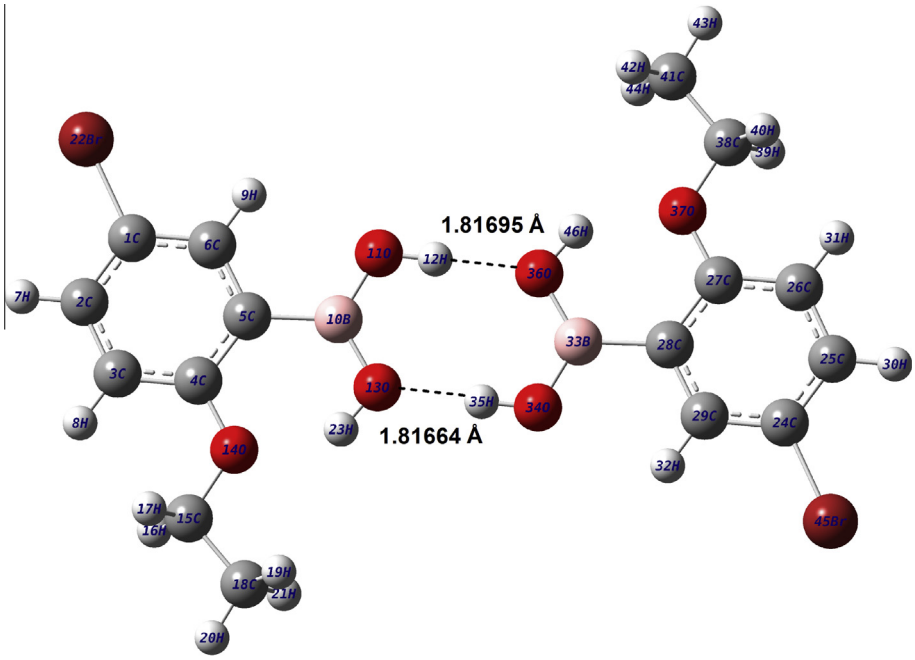

Fig. 2. The theoretical optimized geometric dimer structure of TC conformer of 5Br2EPBA.

Table 2
Bond lengths (Å) and bond angles (°) experimental and optimized of 5Br2EPBA for TC conformer.

Parameters	6-311G(d,p)		6-31G(d)
	Monomer	Dimer	Monomer
Bond lengths (Å)			
C1–C2	1.388	1.388	1.390
C1–C6	1.390	1.389	1.392
C1–Br22	1.921	1.921	1.915
C2–C3	1.394	1.394	1.396
C3–C4	1.396	1.396	1.399
C4–C5	1.411	1.410	1.413
C4–O14	1.375	1.377	1.377
C5–C6	1.400	1.400	1.402
C5–B10	1.576	1.578	1.577
B10–O11	1.367	1.350	1.370
B10–O13	1.363	1.382	1.366
O11–H12	0.963	0.977	0.969
O13–H23	0.966	0.969	0.972
O14–C15	1.434	1.435	1.432
O14–H23	1.918	1.873	1.907
C15–C18	1.517	1.516	1.518
C–H Ring	1.082	1.082	1.084
C–H Ethyl	1.096	1.096	1.098
C–H Methyl	1.092	1.092	1.095
Bond angles (°)			
C2–C1–C6	120.7	120.7	120.6
C2–C1–Br22	119.5	119.5	119.5
C6–C1–Br22	119.8	119.8	119.8
C1–C2–C3	119.5	119.5	119.5
C2–C3–C4	120.0	119.9	119.8
C3–C4–C5	121.1	121.2	121.3
C3–C4–O14	122.6	122.5	122.5
C5–C4–O14	116.4	116.4	116.2
C4–C5–C6	117.7	117.7	117.5
C4–C5–B10	123.6	124.2	123.7
C6–C5–B10	118.7	118.2	118.8
C1–C6–C5	121.1	121.1	121.2
C5–B10–O11	117.3	118.4	117.3
C5–B10–O13	123.9	121.7	123.9
O11–B10–O13	118.8	119.9	118.8
B10–O11–H12	111.4	114.4	110.1
B10–O13–H23	110.4	178.0	109.6
C4–O14–C15	120.0	110.5	119.7
O14–C15–H16	109.4	120.1	109.4
O14–C15–H17	109.4	109.3	109.4
O14–C15–C18	107.6	109.3	107.8
H16–C15–H17	108.4	107.7	108.2
H16–C15–C18	111.0	108.5	111.0
H17–C15–C18	111.0	111.0	111.0
C15–C18–H20	109.9	110.8	109.9
C15–C18–H21	110.8	109.9	110.8
C15–C18–H19	110.8	111.0	110.8
C–C–H Ring	119.9	119.9	119.9
H–C–H Methyl	108.4	109.3	108.4
Intermolecular H bond lengths and angles			
H12···O36	–	1.81695	–
H35···O13	–	1.81664	–
B10–O13···H35	–	127.6	–
H23–O13···H35	–	121.9	–
B12–O36···H33	–	127.6	–
H23–O13···H46	–	121.9	–
H23–O13···H35–O34	–	180.6	–
O11–H12···O36–H46	–	176.9	–
B33–O34–H35···O13	–	−0.6	–
B10–O11–H12···O36	–	3.1	–

However in the dimer structure, these bonds showed differences (1.382 Å and 1.350 Å). This difference can be intermolecular interaction of hydrogen atoms, attached oxygen atoms.

The C–B bond distances are observed at 1.553 Å and 1.545 Å [12] and calculated at 1.566 Å and 1.567 Å [14], for 4-chloro- and 4-bromophenylboronic acid, respectively. The experimental values of phenylboronic acid was observed at 1.568 Å [12]. Bhat et al. [34] calculated B–C bond lengths at 1.566 Å and 1.567 Å in the most stable form for phenylboronic acid, respectively. In this study, the bond distances of B–C show well agreement with structurally similar molecules in the literature [14,15,18–21].

When substituted X (X, F, Cl, Br, etc.) attached in place of hydrogen atom, the C–X bond length shows a considerable increase. The C–Br bond length value is observed at 1.895 Å [12] and calculated at 1.917 Å [14] for 4-bromophenylboronic acid. This bond length is observed at 1.897 Å and 1.904 Å (experimentally) [35] and calculated at 1.917 Å (monomer) and 1.916 Å (dimer) for the similar structures [36]. In this work, the C–Br bond length is calculated at 1.921 Å for monomer and dimer structures by using B3LYP/6-311G(d,p) and 1.915 Å B3LYP/6-31G(d) basis sets showing good coherent related papers [35–37].

The bond angles of the ring (C–C–C) are observed in the range of 117.2–121.8° for phenylboronic acid [9] and 117.6–123.9° for 3-fluorophenylboronic acid [38]. In this study, the CCC bond angles are calculated in the region 117.7–121.1°. The C_4–C_5–C_6 bond angle deviated from normal value is smaller than the others, it can be attached bromine atom in the $B(OH)_2$ group. The other bond angles of the studied molecule are listed in Table 2. The bond angles showed the small difference between the experimental values [9,12], this can be due to calculation belongs to vapor phase and experimental results belong to solid phase. One can quite easily see from Table 2, all the calculations of bond angles are in very consistency with the compared experimental values [14,15,18–21].

The minimum energies of the dimer structure of the title molecule calculated by the DFT/B3LYP/6-31G(d) and 6-311G(d,p) are −6266.45618804 and −6271.65742203 Hartree, respectively. The interaction arises through O–H···O two equivalent stable hydrogen-bonded O11–H12···O36 and O34–H35···O36 contacts, which result in increased stabilization. The O–H distances in the groups involved in the hydrogen bonds are lengthened by 0.014 and 0.003 Å upon dimerization. The shortening of the B10–O11 bond (0.017 Å), while the lengthening of the B10–O13 bond of the title molecule (0.019 Å) upon dimerization, and is due to the redistribution of partial charges.

Vibrational spectral analysis

5Br2EPBA molecule which has C_s point group symmetry has 23 atoms and 63 fundamental vibrational modes TC and TT conformers and C_1 point group symmetry for CT and CC conformers. CT and CC are unstable conformer in C_s point group symmetry due to the imaginary frequencies while, TC and TT are stable in C_s point group symmetry. Due to C_s symmetry point group 63 fundamental vibrational modes are represented by symmetry species $41A' + 22A''$, with the A' representing in-plane motions and A'' representing out-of plane motions. The calculated wavenumbers of the most stable conformer TC are tabulated in Table 3 together with the experimental wavenumbers. A detailed description of the normal modes are performed at the B3LYP method with 6-311G(d,p) and 6-31G(d), basis sets, with their TED given in Table 3 for C_s symmetry point group. The calculated vibrations at the B3LYP method with 6-311G(d,p) for the dimer structure is also presented in Table S2.

The theoretical results are generally higher than the tentative ones; the differences can be a consequence of the anharmonicity and the general tendency of the quantum chemical methods to overestimate the force constants at the exact equilibrium geometry. The theory has been made for free molecule in vacuum, while experiments were performed for solid sample this is the other possibility. This discrepancy partly is fixed with the scaling factor. The theoretical (with the scaling factor for B3LYP/6-311G(d,p)) and experimental FT-IR and FT-Raman spectra are shown in Figs. 3 and 4 for comparative purpose, where the calculated intensity is plotted against harmonic vibrational wavenumbers. This part of the work is to the assignment of the vibrational absorptions to

Table 3
The comparison of calculated harmonic frequencies and experimental (FT-IR and FT-Raman) wavenumbers (cm^{-1}) by using B3LYP method 6-311G(d,p) and 6-311G(d) basis sets for TC conformer's of 5Br2EPBA.

Sym. species	Experimental		B3LYP/6-31G(d)					B3LYP/6-311G(d,p)					Assignments[a]
	FT-IR	FT-Raman	Unscaled	Scaled	I_{IR}	S_{Ra}	I_{Ra}	Unscaled	Scaled	I_{IR}	S_{Ra}	I_{Ra}	TED (⩾10%)
A″			41	39	0.15	0.98	1088.49	37	35	0.10	0.92	1261.07	ΓCCCO (57), ΓCOCH (32)
A″			56	53	0.37	0.10	61.84	60	58	0.10	0.07	38.21	$tB(OH)_2$ {ΓCCBO (84)}
A″		91vs	96	92	2.31	0.50	113.15	95	92	2.59	0.49	111.82	ΓCCOC (53)
A′			121	116	0.26	0.19	27.96	119	114	0.24	0.17	26.55	δCCO (75), δCCBr (17)
A″			129	124	0.22	0.78	101.94	124	119	0.30	1.03	144.66	ΓCOCH (29), ΓCCCO (25), ΓCCCBr (20)
A′			131	125	1.07	1.13	145.62	129	124	1.13	1.12	147.30	δCCBr (51) {$rB(OH)_2$}, δCCB (42)
A″		153vs	142	137	0.03	2.05	226.66	140	134	0.00	1.83	209.07	ΓCBCO (40), ΓCCCBr (21), ΓCCCB (15)
A′			244	234	1.70	8.22	363.68	242	233	1.63	8.51	379.79	υCBr (45), δCCC (18)
A″		249vs	259	249	0.89	0.01	0.30	262	251	0.74	0.00	0.09	ωCH_3 (95)
A′			277	266	5.83	0.33	12.04	275	264	5.19	0.39	14.36	δCCBr (31), δCBO (28), δCCO (17)
A″			329	316	2.30	2.20	60.47	327	314	0.07	1.06	29.35	ΓCCCBr (28), ΓCCCO (23), ΓCBrCH (19), ΓCCCO (15)
A′			333	320	0.03	1.46	39.12	327	315	2.13	2.23	61.65	υCB (25), δCBO (21), δCCO (17)
A′		329w	345	331	2.51	1.00	25.53	344	330	2.54	1.03	26.46	δCBO (32), δCCO (18)
A′		358w	413	397	1.41	0.66	12.79	412	396	1.54	0.68	13.19	δCCO (43), υCBr (15)
A″		425vw	425	408	6.6	0.86	16	421	405	7.01	0.74	13.98	ΓCCCC (42), ΓCCCH (13)
A′			525	504	23.74	2.95	40.07	525	504	24.72	2.94	39.93	δOBO (35), δCBO (27)
A″	525s		532	511	1.60	2.36	31.45	527	506	0.01	1.66	22.44	ΓCCCC (28), ΓCCCH (24), ΓCBOH (17)
A″	531w		562	539	140.2	2.28	28.07	556	535	127.77	2.03	25.27	γOH (65)
A′	572w	537vw	566	543	6.70	1.15	13.98	564	542	7.91	0.94	11.43	δCBO (34), δCCO (34)
A′			656	630	23.39	6.33	62.32	655	630	25.09	6.32	62.28	δCCC (42), δCCO (22)
A″	636s	643s	659	633	29.4	0.35	3.39	663	637	26.33	0.33	3.19	γOH (66), ΓCCCC (12)
A″	679s		673	646	51.46	0.54	5.17	679	652	45.60	0.50	4.64	γOH (88)
A′			744	715	29.35	6.96	57.08	743	714	30.19	7.08	58.25	υCC (27), υCO (25), δCCC (22), rCH_3 (18)
A″	729s	735w	759	729	8.23	0.16	1.26	758	729	16.18	0.20	1.63	γOH {ΓCBOH (41), ΓCBCO (19)}, ΓCCCC (20)
A″	769s		819	786	34.17	2.04	14.6	816	784	44.41	0.77	5.55	γCH (65), rCH_3 (12)
A′	800s	821s	834	800	9.56	10.27	71.57	832	799	10.30	10.50	73.33	δCCC (33), υCO (20), rCH_3 (15)
A″	810w		851	817	2.38	0.01	0.10	844	811	3.65	0.09	0.62	rCH_3 (48), γCH (40), rCH_2 (11)
A″			945	907	8.92	2.62	15.22	935	899	3.47	0.09	0.53	γCH (83)
A′			955	917	2.56	0.86	4.93	938	901	10.56	2.84	16.62	υCC (29), υCO (17), rCH_3 (16)
A″	918w	938vw	963	925	2.99	1.16	6.52	955	918	1.55	0.32	1.84	γCH (80)
A′			1029	988	146.06	5.82	29.73	1021	981	151.26	5.78	29.83	δBOH (45), υBO (42)
A′	1018vs	1015vw	1065	1022	79.59	3.63	17.58	1054	1012	78.44	6.04	29.72	υCC (36), υCO (31), δBOH (13)
A′	1042vs		1092	1049	81.55	4.26	19.89	1084	1042	87.32	3.29	15.50	δBOH (32), υCC (21), υCO (11)
A′			1113	1068	17.04	9.02	40.87	1102	1059	18.57	10.02	45.99	υCC (53), δCCHring (20) Ring breathing
A′	1073w	1098w	1133	1088	19.16	12.54	55.23	1126	1082	19.96	12.65	56.16	δBOH (40), υCC (11)
A′			1153	1108	25.77	1.94	8.31	1141	1097	21.61	1.62	7.03	rCH_3 (29), υCC (12), δBOH (11)
A′	1118s		1189	1142	61.67	8.10	33.10	1177	1131	63.11	8.04	33.32	δCCHring (56), υCC (17)
A″	1153vs	1147vw	1195	1147	3.89	2.12	8.60	1181	1135	3.85	1.21	4.99	tCH_2 (44), tCH_3 (46)
A′			1266	1216	267.1	9.05	33.48	1248	1199	257.99	11.28	42.63	υCO (47), υCC (21)
A′	1229vs	1233w	1305	1254	5.39	0.87	3.07	1291	1241	8.15	0.50	1.80	δCCHring (51), υCC (14)
A″			1315	1263	0.49	13.76	47.83	1305	1254	0.84	8.13	28.58	tCH_2(70), rCH_3 (20)
A′	1267s	1270w	1330	1278	32.71	9.54	32.53	1308	1257	26.55	9.90	34.68	Ring deformation.{υCC (82)}
A′	1311vs		1379	1324	287.67	7.93	25.51	1362	1309	281.46	6.73	22.04	υBOsym. (25), δCCHring (15), δBOH (13), υCC (13)
A′			1416	1360	140.19	2.04	6.27	1399	1345	121.27	1.26	3.95	τCH_3 (33), rCH_2 (20), υBO (11)
A′			1423	1367	193.87	3.03	9.22	1405	1351	169.82	2.49	7.74	υBOsym. (23), rCH_2 (15), τCH_3 (15), δBOH(11), υCC (11)
A′			1449	1392	89.83	6.79	20.08	1426	1371	100.76	3.37	10.21	τCH_3 (40), rCH_2 (28)
A′	1384vs	1408vw	1464	1405	179.76	4.94	14.36	1446	1390	190.09	4.03	11.96	υBOasym. (45), υCC (21)
A″	1434s		1516	1456	6.48	23.68	64.79	1488	1430	8.14	13.71	38.71	ρCH_3 (80)
A′		1461w	1519	1459	186.43	2.80	7.62	1499	1441	190.69	2.62	7.29	δCCHring (22), υCC (17), ρCH_2 (15)
A′			1530	1470	2.81	20.55	55.29	1505	1446	6.96	12.89	35.68	ρCH_3 (44), ρCH_2 (20), δCCHring (11)
A′	1471vs	1485vw	1556	1494	2.62	4.71	12.31	1529	1470	5.91	4.74	12.75	ρCH_3 (36), ρCH_2 (27)
A′			1619	1555	20.54	9.44	23.00	1601	1539	20.68	8.27	20.51	υCCring (68)
A′	1590s	1590s	1643	1578	54.25	39.33	93.33	1626	1562	57.07	38.14	92.11	υCCring (64)

A′		3030	2909	29.75	83.78	51.07	3009	2892	29.74	99.79	61.84	υCH$_2$sym. (100)
A′		3063	2941	14.74	125.22	74.02	3039	2921	15.57	154.19	92.97	υCH$_3$sym. (100)
A″		3070	2948	27.71	59.36	34.85	3049	2930	22.69	66.44	39.70	υCH$_2$asym. (96)
A′	2930w	3136	3012	21.41	97.48	53.86	3109	2988	22.99	102.16	57.75	υCH$_3$asym. (100)
A″	2979s	3139	3014	26.36	41.97	23.13	3113	2991	28.14	42.15	23.75	υCH$_3$asym. (96)
A′	2988vw	3218	3091	3.66	51.43	26.34	3195	3070	2.49	54.61	28.53	υCH (100)
A′	3070w	3231	3103	0.46	34.80	17.62	3206	3081	0.50	38.76	20.04	υCH (98)
A′		3236	3107	9.13	138.79	69.97	3213	3088	7.39	141.78	72.83	υCH (98)
A′	3371vs	3709	3562	188.63	34.13	11.12	3768	3621	208.89	31.25	9.61	υOH(O$_{12}$–H$_{13}$) (100)
A′		3773	3623	56.63	190.46	58.50	3849	3699	76.02	181.89	51.89	υOH(O$_{11}$–H$_{23}$) (100)

[a] υ; stretching, δ; in-plane bending, ρ; scissoring, r; rocking, τ; umbrella, t; twisting γ; out of plane bending Γ; torsion, ω; wagging, sym.; symmetric, asym.; asymmetric, I_{IR}, IR intensity; S_{Ra}, Raman scattering activity; I_{Ra}, Raman intensity.

make a comparison with the results obtained from the theoretical calculations and the structurally similar molecules.

The assignment of the O–H stretching vibrations is pure and apprehensible. The O–H stretching vibrations in derivatives of boronic acids in the solid state absorb broadly near 3300–3200 cm^{-1} and are extremely sensitive to formation of hydrogen bonding. The band O–H were observed at 3280 cm^{-1} in IR (phenylboronic acid) [13], at 3276, 3249 cm^{-1} and 3276, 3164 cm^{-1} in FT-IR (4-chloro-) and at 3175, 3106 and 3108 cm^{-1} in FT-Raman (4-bromo phenylboronic acid) [14], at 3443, 3397 cm^{-1} in FT-IR, at 3480, 3440 cm^{-1} in FT-Raman and 3465, 3425 cm^{-1} in FT-IR (3,4 and 3,5 dichlorophenylboronic acid) [16,17]. This band is observed at 3400 and 3332 cm^{-1} in FT-IR spectrum and predicted at 3685 (O_7–H_{11}) and 3692 cm^{-1} (O_8–H_{10}) for 2,3-difluorophenylboronic acid in the prior work [19]. The O–H stretching modes were calculated at 3610 and 3334 cm^{-1} as expected pure stretching modes accordance TED contributing 100% and observed at 3551 and 3250 cm^{-1} FT-IR [36]. In this study, the O–H stretching modes of 5Br2EPBA molecule are observed at 3371(vs) cm^{-1} in FT-IR spectrum and predicted at 3699 cm^{-1} (O_{11}–H_{23}) and 3621 (O_{12}–H_{13}). The OH in-plane bending modes are calculated at 1082, 1042, 981 cm^{-1}. This band is observed at 1098 cm^{-1} in FT-Raman and at 1073, 1042 cm^{-1} in FT-IR. The OH out-of-plane bending modes are computed at 535, 637, and 652 cm^{-1} for the title molecule. This band at 531, 636, 679 cm^{-1} in FT-IR and at 643 cm^{-1} in FT-Raman band is assigned the OH out-of-plane bending. Theoretical values of the OH bending vibrations are good coherent in experimental values. The O–H stretching modes in dimeric structure of the title molecule are decreasing and the values of O–H in plane and out-of-plane bending vibrations in dimer (came from δBOH and γOH) conformation are changing in ascending or descending direction, because of the hydrogen-bonding effect through the B(OH)$_2$ group (Table S2).

The C–H stretching modes as multiple peaks seem in the 3000–3100 cm^{-1} range which is the characteristic region. The in plane bending and out-of-plane bending modes of C–H vibrations appear in the range of 1000–1300 cm^{-1} and in the region 750–1000 cm^{-1} [39]. In literature [14–17,19], the C–H stretching modes were predicted in the range of 3030–3100 cm^{-1} for structurally similar compounds. In this study, the C–H stretching vibrations are calculated in the region 3088–3070 cm^{-1} for ring CH by using the B3LYP/6-311G(d,p) method. This mode is observed at 3070 cm^{-1} in FT-Raman. All of them are very pure modes based on their TED contribution (ca. 100%). The C–H in-plane bending vibrations are predicted very wide range nearly 1441, 1309, 1241, 1131, and 1059 cm^{-1} and observed at 1311, 1229, and 1118 cm^{-1} in FT-IR, 1461 and 1233 cm^{-1} in FT-Raman. The C–H out of plane bending modes are predicted at 918, 899, 811, 784, and 506 cm^{-1}, respectively. These modes are observed at 918, 810, 769, 525 cm^{-1} in FT-IR, at 938 cm^{-1} in FT-Raman, respectively. The TED results showed that the out-of plane modes have been also highly pure modes like in-plane bending fundamental. The bending vibrations (both in-plane and out-of plane) are contaminated other modes, especially CC stretching modes. Theoretical and experimental data for CH bending modes show very good correlation with each other and structurally similar molecules [13,15–21].

The spectral position of C–H stretching of the methyl and methylene groups is at lower frequencies than those of the aromatic C–H ring stretching. The CH_3 and CH_2 anti-symmetric stretching vibrations are generally observed in the region 3100–2900 cm^{-1}, while the symmetric stretch will appear between 2900 and 2800 cm^{-1}. The CH_3 and CH_2 asymmetric stretching vibrations are observed at 2988 and 2930 cm^{-1}, respectively in FT-Raman. The symmetric stretching vibrations are also observed in FT-IR at 2925 cm^{-1} and 2889 cm^{-1} as CH_3 and CH_2 symmetric stretching modes, respectively. Out of four types of bending motions namely scissoring, twisting, wagging and rocking of methyl and methylene

groups are observed and calculated (see Table 3). Theoretical values of ring CH, CH_3 and CH_2 stretching and bending vibrations are good coherent in experimental values.

The B–O vibration mode is very intense and includes the symmetric and asymmetric stretching vibrations. The asymmetric mode is located at 1350 cm^{-1} in infrared spectrum for phenylboronic acid [13] and at 1375 cm^{-1} for the phenylboronic acid linkage [40]. The νB–O modes are recorded at 1373 and 1361 cm^{-1} by Kurt [14] for 4-chlorophenylboronic acid and 4-bromophemylboronic acid, respectively. These modes also were calculated at 1400–1350 cm^{-1} using B3LYP method [16,17,33]. The νB–O stretching vibrations were calculated at 1345, 1371 and 1002 cm^{-1} by using B3LYP method assigned as two symmetric and asymmetric modes for derivative of the phenyl boronic acid and observed at 1352 and 1351, 1389 cm^{-1} in FT-IR and FT-Raman spectra [19]. In this study, the B–O asymmetric and symmetric stretching modes are calculated at 1390, 1351 and 1309 cm^{-1} by using B3LYP/6-311G(d,p). The B–O stretching bands are observed at 1384 (asym.) and 1311 (sym.) cm^{-1} in FT-IR, at 1408 (asym.) cm^{-1} in FT-Raman, respectively. These modes are nearly a pure mode according to their TED calculations see in Table 3. The B–O–H bending and torsion modes of with the ring and boronic acid groups (except for identified as OH/CH in plane and out-of plane) are mixed the other modes also assigned by their TED if anyone see in Table 3. The OH or related the interaction modes are different with the each other. The in-plane BO_2 mode has been observed as a doublet at 502 cm^{-1} for, 3,5-difluorophenylboronic acid [19], in the present calculation we have assigned this mode at 504 cm^{-1} with 35% TED to be the in-plane BO_2 mode.

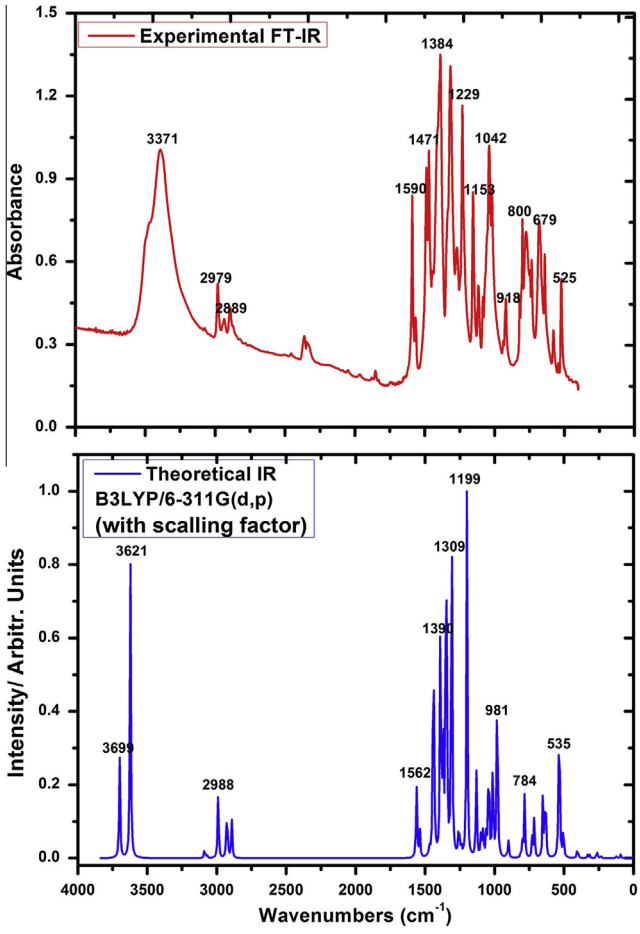

Fig. 3. The experimental and calculated (with the scale factor) infrared spectra of 5Br2EPBA.

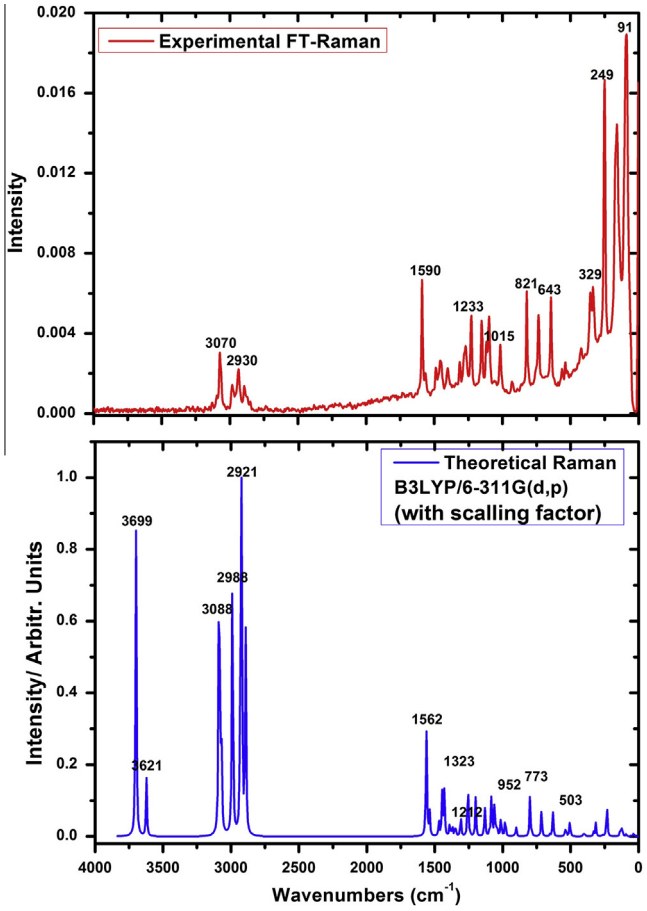

Fig. 4. The experimental and calculated (with the scale factor) Raman spectra of 5Br2EPBA.

The other highly characteristic and very much important modes are C–C stretching vibrations for the aromatic ring. Varsanyi [41] have been observed at 1625–1590, 1590–1575, 1540–1470, 1465–1430 and 1380–1280 cm^{-1} from the frequency ranges for the five bands in the region as variable intensity. The C–C stretching vibrations of phenylboronic acid were assigned in the range of 1620–1320 cm^{-1} [13]. Similarly, the C–C stretching modes were recorded for 4-bromophenylboronic acid in the region 1590–1010 cm^{-1} and 1588–1004 cm^{-1} in FT-IR and FT-Raman, for 4-chlorophenylboronic acid in the range of 1596–1060 cm^{-1} and 1588–1085 cm^{-1} in FT-IR and FT-Raman, respectively [14], 2-fluorophenylboronic acid at the range of 1617–1034 cm^{-1} (IR) [33], supported DFT calculations computed ca. 1650–990 cm^{-1} using B3LYP calculations [16,17]. In the present paper, the C–C stretching vibrations are calculated at 1562, 1539, 1441, 1390, 1309, 1241, 1199, 1131–1012, 901, and 714 cm^{-1} for TC conformer of the studied molecule, by using the hybrid B3LYP level of theory with the 6-311G(d,p) basis set. Experimental ones are 1590, 1384, 1311, 1229, 1118, and 1073–1018 cm^{-1} in FT-IR and 1590, 1461, 1408, 1233, 1098, and 1015 cm^{-1} in FT-Raman, respectively. The C–C stretching as main vibrations are calculated at 1562 and 1539 cm^{-1}, seen pure modes with the TED contribution 64% and 68%, respectively. The C–C modes at 1257 and 1059 cm^{-1} are assigned (1267 cm^{-1} in FT-IR) as a ring deformation and ring breathing modes. The other torsion (except as specifically assigned) and CCC bending modes contaminated with other modes and are obtained in a large region. The dominant CCC bending mode is observed at 800 and 821 cm^{-1} in FT-IR and FT-Raman; calculated wavenumber of this mode coincide at as 799 cm^{-1} after scaling.

In the bromine compounds, the C–Br stretching mode appears at longer wavelength region 200–480 cm^{-1} is reported by Varsanyi [41]. The theoretical wavenumbers of the C–Br stretching vibration coupled with other group vibrations. According to the calculated TED, there is no pure C–Br band vibration. In previous study, this band at 283 cm^{-1} (FT-Raman) is assigned to C–Br stretching vibration coupled with ring deformation (mode 37). The theoretical wavenumber of this band is computed at 285 cm^{-1} and its TED is 50%. Moreover, the calculated at 625 and 275 cm^{-1} involve some contribution from the C–Br stretching vibration [36]. The C–Br stretching vibration modes were calculated at 547 and 389 cm^{-1} using B3LYP method for 4-bromophenylboronic acid [14]. In this study, we also recorded the mode of C-Br at 358 cm^{-1} in FT-Raman spectrum and calculated theoretically at 396 and 233 cm^{-1} by using B3LYP/6-311G(d,p) basis set. At the glance of the C–Br stretching modes; they are very good agreement with the experimental and literature results. The C–Br in-plane bending and out-of-plane bending modes appear in variable region according to molecular structure and state of the bromine substituent. According to TED, the C–Br in plane bending vibrations are calculated at 264 and 124 cm^{-1}. The C–Br out-of-plane bending vibrations are also calculated at 314, 134, and 119 cm^{-1}, observed at 153 cm^{-1} in FT-Raman. This is in agreement with the literature data [14,36,41,42]. The remainder bending and torsion modes of the related bromine atom accounted in Table 3.

To see correlation between calculated and experimental wavenumbers, the correlation graphic are plotted in Fig. S2. The experimental fundamentals have a better correlation with the theoretical results as shown in Fig. S2. The correlations of infrared and Raman are graphed severally in Fig. S3(a)–(b). The following equations are described relations between the calculated and experimental wavenumbers as linear;

$$\nu_{cal} = 1.0187\nu_{exp} - 17.537 \quad (\text{Total} - R^2 = 0.9981)$$

$$\nu_{cal} = 1.0341\nu_{exp} - 38.219 \quad (\text{Infrared} - R^2 = 0.9974)$$

$$\nu_{cal} = 0.9988\nu_{exp} - 4.9995 \quad (\text{Raman} - R^2 = 0.9998)$$

NBO analysis

NBO analysis provides the most accurate possible 'natural Lewis structure' picture of φ, because all orbital details are mathematically chosen to include the highest possible percentage of the electron density. A useful aspect of the NBO method is that it gives information about interactions in both filled and virtual orbital spaces that could enhance the analysis of intra- and intermolecular interactions. The second-order Fock matrix was carried out to evaluate the donor–acceptor interactions in the NBO analysis [43].

NBO analysis has been carried out to explain the charge transfer or delocalization of charge due to the intra-molecular interaction among bonds, and also provides a convenient basis for investigating charge transfer or conjugative interaction in molecular systems. Some electron donor orbital, acceptor orbital and the interacting stabilization energy resulting from the second-order micro disturbance theory is reported [44,45]. The larger the stabilization energy value, the more intensive is the interaction between electron donors and electron acceptors, i.e. the more donating tendency from electron donors to electron acceptors and the greater the extent of conjugation of the whole system. Delocalization of electron density between occupied Lewis-type (bond or lone pair) NBO orbitals and formally unoccupied (anti bond or Rydberg) non-Lewis NBO orbitals correspond to a stabilizing donor–acceptor interaction.

NBO calculation is performed by using Gaussian09 package program at the DFT/B3LYP level in order to understand various second-order interactions between the filled orbitals of one subsystem and vacant orbitals of another subsystem, which is a measure of the delocalization or hyper conjugation. The corresponding results have been tabulated in Tables 4 and 5.

The intramolecular interactions are observed as increase in electron density (ED) in (C–C) anti-bonding orbital that weakens the respective bonds. The electron density of conjugated bond of aromatic ring (1.97 e) clearly demonstrates strong delocalization. The occupancy of π bonds is lesser than σ bonds which lead more delocalization.

The intramolecular hyperconjugative interaction of the σ(C1–C2) distribute to σ*(C1–C6) and (C2–C3) leads to less stabilization of 3.92 and 3.44 kJ/mol, respectively. This enhanced further conjugate with antibonding orbital of π*(C3–C4) and (C5–C6) which leads to strong delocalization of 15.71 and 22.40 kJ/mol, respectively. This enhanced π*(C1–C2) NBO further conjugates with π*(C5–C6), resulting in an enormous stabilization energy of 165.76 kJ/mol, as shown in Table 5.

As in the case of the O–H bond, σ(O11–H12) and σ(O13–H23) conjugation with σ*(C5–B10) and σ*(B10–O11) leads to less stabilization energy of 2.54 and 3.65 kJ/mol, respectively. These shows that the σ(O–H) bonds do not have the stability to cause any change in the phenyl ring.

NMR analysis

The chemical shift analysis is one of the most important techniques for the structural analysis for organic compounds. Firstly, the molecular structure of 5Br2EPBA molecule is optimized. Then, ^{1}H and ^{13}C NMR chemical shifts calculations of 5Br2EPBA molecule are carried out by using GIAO method and B3LYP functional with 6-31G(d) and 6-311G(d,p) basis sets. The GIAO [30,31] approach to molecular systems is substantially evolved by an efficient application of the method to the ab initio SCF calculations, by using techniques taken from analytic derivative methodologies. The calculations reported in DMSO solution and gas phase, rather than in the gas phase, are in agreement with experimental chemical shifts obtained in DMSO. The experimental ^{1}H, ^{13}C, and DEPT NMR spectra of the title molecule are given in Fig. 5a–c, respectively. The experimental and theoretical ^{1}H and ^{13}C chemical shifts for monomer and dimer structures in DMSO are listed in Table 6. The atom positions are listed according to Fig. 1.

The title molecule has ten hydrogen atoms as attached to aromatic ring, two hydrogen atoms attached to the oxygen atoms of boronic group, and ethoxy group (CH_3CH_2O–). The aromatic protons of organic molecules are usually recorded in the range of 7.00–8.00 ppm. However, the proton chemical shift of organic molecules varies greatly with the electronic environment of the proton. Hydrogen attached or nearby electron-donating atom or group increases the shielding and moves the resonance towards to a lower frequency, whereas electron-withdrawing atom or group can decrease the shielding and move the resonance of attached proton towards to a higher frequency [46]. Aromatic ring protons are founded this range experimentally see Table 6, and Fig. 5a. The experimental isotropic chemical shifts of protons are observed at 6.94, 7.50, and 7.59 (aromatic ring), 1.33, 1.35, 1.36, 4.04, and 4.06 (ethoxy group), 7.86 (boronic group) ppm. Theoretical values are recorded in the region parts as nearly the same ppm for monomer and dimer structures. We have calculated ^{1}H NMR chemical shift values (with respect to TMS) of 1.72–8.07 ppm and 1.32–7.87 ppm at B3LYP/6-31G(d) and B3LYP/6-311G(d,p) levels in DMSO, respectively. The experimental shifts are observed at 1.33–7.86 ppm. The H13 value was computed smaller than H23 chemical shifts it can be due to the electronic environment of the

Table 4
NBO results showing formation of Lewis and non-Lewis orbitals for 5Br2EPBA.

Bond (A–B)	Type	ED/energy (a.u.)	ED_A (%)	ED_B (%)	NBO	s (%)	p (%)
C1–C2	σ	1.98	49.76	50.24	$0.7054(sp^{1.55})C + 0.7088(sp^{1.74})C$	39.17	60.78
		−0.731				36.47	63.49
C1–C6	σ	1.98	50.04	49.96	$0.7074\ (sp^{1.52})C + 0.7069(sp^{1.76})C$	39.69	60.26
		−0.727				36.27	63.69
C1–Br22	σ	1.982	48.53	51.47	$0.6966(sp^{3.73})C + 0.7174(sp^{5.85})Br$	21.11	78.77
		−0.647				14.54	85.06
C2–C3	σ	1.965	49.85	50.15	$0.7060(sp^{1.80})C + 0.7082(sp^{1.74})C$	35.69	64.26
		−0.705				36.42	63.54
C3–C4	σ	1.979	50.03	49.97	$0.7073(sp^{1.82})C + 0.7069(sp^{1.60})C$	35.45	64.50
		−0.719				38.38	61.58
C4–C5	σ	1.969	50.09	49.91	$0.7078(sp^{1.65})C + 0.7065(sp^{1.96})C$	37.75	62.22
		−0.7				33.72	66.23
C4–O14	σ	1.99	31.46	68.54	$0.5609(sp^{3.22})C + 0.8279(sp^{1.93})O$	23.64	76.13
		−0.908				34.06	65.88
C5–C6	σ	1.961	50.5	49.5	$0.7107(sp^{1.91})C + 0.7035(sp^{1.78})C$	34.39	65.57
		−0.69				35.99	63.97
C5–B10	σ	1.961	68.09	31.91	$0.8252(sp^{2.13})C + 0.5649(sp^{1.52})B$	31.99	67.99
		−0.52				39.62	60.35
B10–O11	σ	1.995	20.72	79.28	$0.4552(sp^{2.40})B + 0.8904(sp^{1.18})O$	29.38	70.44
		−0.907				45.84	54.09
B10–O13	σ	1.996	20.92	79.08	$0.4574(sp^{2.23})B + 0.8892(sp^{1.26})O$	30.86	68.92
		−0.902				44.23	55.71
O14–C15	σ	1.99	69.31	30.69	$0.8326(sp^{2.43})O + 0.5539(sp^{3.85})C$	29.11	70.84
		−0.834				20.57	79.15
C15–C18	σ	1.986	50.57	49.43	$0.7111(sp^{2.25})C + 0.7030(sp^{2.39})C$	30.75	69.20
		−0.65				29.52	70.44
C1–C2	σ*	0.028	50.24	49.76	$0.7088(sp^{1.55})C - 0.7054(sp^{1.74})C$	39.17	60.78
		0.569				36.47	63.49
C1–C6	σ*	0.029	49.96	50.04	$0.7069(sp^{1.52})C - 0.7074(sp^{1.76})C$	39.69	60.26
		0.578				36.27	63.69
C1–Br22	σ*	0.038	51.47	48.53	$0.7174(sp^{3.73})C - 0.6966(sp^{5.85})Br$	21.11	78.77
		0.092				14.54	85.06
C2–C3	σ*	0.017	50.15	49.85	$0.7082(sp^{1.80})C - 0.7060(sp^{1.74})C$	35.69	64.26
		0.568				36.42	63.54
C3–C4	σ*	0.03	49.97	50.03	$0.7069(sp^{1.82})C - 0.7073(sp^{1.60})C$	35.45	64.50
		0.553				38.38	61.58
C4–C5	σ*	0.028	49.91	50.09	$0.7065(sp^{1.65})C - 0.7078(sp^{1.96})C$	37.75	62.22
		0.554				33.72	66.23
C4–O14	σ*	0.035	68.54	31.46	$0.8279(sp^{3.22})C - 0.5609(sp^{1.93})O$	23.64	76.13
		0.34				34.06	65.88
C5–C6	σ*	0.021	49.5	50.5	$0.7035(sp^{1.91})C - 0.7107(sp^{1.78})C$	34.39	65.57
		0.575				35.99	63.97
C5–B10	σ*	0.032	31.91	68.09	$0.5649(sp^{2.13})C - 0.8252(sp^{1.52})B$	31.99	67.99
		0.475				39.62	60.35
B10–O11	σ*	0.021	79.28	20.72	$0.8904(sp^{2.40})B - 0.4552(sp^{1.18})O$	29.38	70.44
		0.488				45.84	54.09
B10–O13	σ*	0.022	79.08	20.92	$0.8892\ (sp^{2.23})B - 0.4574(sp^{1.26})O$	30.86	68.92
		0.487				44.23	55.71
O14–C15	σ*	0.029	30.69	69.31	$0.5539(sp^{2.43})O - 0.8326(sp^{3.85})C$	29.11	70.84
		0.261				20.57	79.15
C15–C18	σ*	0.007	49.43	50.57	$0.7030(sp^{2.25})C - 0.7111(sp^{2.39})C$	30.75	69.20
		0.371				29.52	70.44
O11	LP(1)	1.97			$sp^{1.90}$	34.52	65.44
		−0.538					
O13	LP(1)	1.965			$sp^{1.98}$	33.55	66.41
		−0.531					
O14	LP(1)	1.953			$sp^{1.72}$	36.81	63.17
		−0.57					
Br22	LP(1)	1.994			$sp^{0.17}$	85.68	14.31
		−0.971					

H13 atom (the electronic charge density around of H13) for the structure of the title molecule. The signals of the three aromatic ring proton of the 5Br2EPBA molecule are calculated 7.07–8.07 ppm with B3LYP/6-31G(d), 6.82–7.87 ppm (monomer) and 6.45–8.12 ppm (dimer) with B3LYP/6-311G(d,p), respectively. The calculated proton NMR chemical shifts both monomer structure and dimer structures show moderate agreement with experimental values.

Generally, aromatic carbons give resonances in overlapped areas of the spectrum with chemical shift values from 100 to 150 ppm [47,48]. In our present investigation, there are eight different carbon atoms, which are attached phenyl ring and ethoxy group in the present molecule. C6, C2 and C3 atoms appeared at 137.58, 134.14 and 114.36 ppm, respectively can be observed in DEPT NMR spectrum (Fig. 5c) of the title molecule as expected, since those carbon atoms which contain hydrogen bond. Because of hydrogen bond of ethoxy group, the chemical shifts of C15 and C18 atoms are observed at 64.35 and 14.93 ppm, respectively (see Fig. 5c). The chemical shifts of aromatic carbon atoms (from C_1 to C_6) of the headline molecule are calculated at 134.00, 140.04, 114.59, 169.93, 124.18, 143.41 ppm for monomer structure and 134.21, 140.03, 114.72, 169.87, 124.68 and 143.59 ppm for

Table 5
Second order perturbation theory analysis of Fock matrix in NBO basis for 5Br2EPBA.

Donor (i)	Type	ED/e	Acceptor (j)	Type	ED/e	$E^{(2)}$ (kJ mol^{-1})[a]	$E(j) - E(i)$ (a.u)[b]	$F(i,j)$ (a.u)[c]
C1–C2	σ	1.98	C1–C6	σ*	0.029	3.92	1.31	0.064
			C2–C3	σ*	0.017	3.44	1.3	0.06
C1–C2	π	1.69	C3–C4	π*	0.382	15.71	0.29	0.061
			C5–C6	π*	0.33	22.40	0.31	0.074
C1–C6	σ	1.98	C1–C2	σ*	0.028	3.85	1.3	0.063
			C5–C6	σ*	0.021	3.75	1.3	0.062
			C5–B10	σ*	0.032	1.85	1.2	0.042
C1–Br22	σ	1.982	C2–C3	σ*	0.017	3.15	1.22	0.055
			C5–C6	σ*	0.021	3.25	1.22	0.056
C2–C3	σ	1.965	C1–C2	σ*	0.028	4.27	1.27	0.066
			C1–Br22	σ*	0.038	5.56	0.8	0.059
			C3–C4	σ*	0.03	3.6	1.26	0.06
			C4–O14	σ*	0.035	4.53	1.05	0.061
C3–C4	σ	1.979	C2–C3	σ*	0.017	3.44	1.29	0.059
			C4–C5	σ*	0.028	5.15	1.27	0.072
			C5–B10	σ*	0.032	2.19	1.19	0.046
C3–C4	π	1.662	C1–C2	π*	0.388	23.67	0.29	0.074
			C3–C4	π*	0.382	0.52	0.29	0.011
			C5–C6	π*	0.33	15.91	0.3	0.062
C4–C5	σ	1.969	C3–C4	σ*	0.03	4.63	1.25	0.068
			C5–C6	σ*	0.021	3.92	1.27	0.063
			C5–B10	σ*	0.032	2.55	1.17	0.049
			O14–C15	σ*	0.029	3.58	0.96	0.052
			C4–O14	σ*	0.035	0.89	1.04	0.027
C4–O14	σ	1.99	C2–C3	σ*	0.017	1.18	1.48	0.037
			C3–C4	σ*	0.03	0.81	1.46	0.031
			C4–C5	σ*	0.028	0.92	1.46	0.033
			C5–C6	σ*	0.021	1.64	1.48	0.044
			C15–C18	σ*	0.007	0.79	1.28	0.028
C5–C6	σ	1.961	C1–C6	σ*	0.029	4.3	1.27	0.066
			C1–Br22	σ*	0.038	5.49	0.78	0.059
			C4–C5	σ*	0.028	3.85	1.24	0.062
			C4–O14	σ*	0.035	4.24	1.03	0.059
			C5–B10	σ*	0.032	2.63	1.17	0.049
			B10–O13	σ*	0.022	0.65	1.18	0.025
C5–C6	π	1.658	C1–C2	π*	0.388	18.9	0.27	0.064
			C3-C4	π*	0.382	24.67	0.27	0.073
			C5–C6	π*	0.33	0.58	0.28	0.012
C5–B10	σ	1.961	C1–C6	σ*	0.029	4.72	1.1	0.064
			C3–C4	σ*	0.03	4.92	1.07	0.065
			C4–C5	σ*	0.028	1.98	1.07	0.041
			C4–O14	σ*	0.035	1.18	0.86	0.029
			C5–C6	σ*	0.021	2.41	1.1	0.046
			B10–O11	σ*	0.021	0.65	1.01	0.023
B10–O11	σ	1.995	C4–C5	σ*	0.028	1.42	1.46	0.041
B10–O13	σ	1.996	C5–C6	σ*	0.021	0.91	1.48	0.033
			C5–B10	σ*	0.032	0.61	1.38	0.026
O14–C15	σ	1.99	C4–C5	σ*	0.028	2.5	1.39	0.053
C15–C18	σ	1.986	C4–O14	σ*	0.035	3.18	0.99	0.05
C1–C2	π*	0.388	C5–C6	π*	0.33	165.76	0.02	0.083
C3–C4	π*	0.382	C5–C6	π*	0.33	162.42	0.02	0.083
O11–H12	σ	1.986	C5–B10	σ*	0.032	2.54	1.2	0.049
O13–H23	σ	1.985	B10–O11	σ*	0.021	3.65	1.22	0.06
B10	LP(1)*	0.39	C5–C6	π*	0.33	104.76	0.02	0.073
O13	LP(1)	1.965	C5–B10	σ*	0.032	5.76	1.01	0.068
			B10–O11	σ*	0.021	2.95	1.02	0.049
O14	LP(1)	1.953	C3–C4	σ*	0.03	6.19	1.12	0.075
			C4–C5	σ*	0.028	0.52	1.12	0.022
			C15–C18	σ*	0.007	1.12	0.94	0.029
	LP(2)	1.856	C3–C4	π*	0.382	27.54	0.35	0.094
Br22	LP(1)	1.994	C1–C2	σ*	0.028	1.49	1.54	0.043
			C1–C6	σ*	0.029	1.52	1.55	0.044
	LP(2)	1.976	C1–C2	σ*	0.028	3.32	0.86	0.048
			C1–C6	σ*	0.029	3.33	0.87	0.048
	LP(3)	1.944	C1–C2	π*	0.388	9.18	0.3	0.052
O11	LP(1)	1.97	C5–B10	σ*	0.032	2.22	0.99	0.042
			B10–O13	σ*	0.022	5.3	1.03	0.066

[a] $E^{(2)}$ means energy of hyperconjugative interactions.
[b] Energy difference between donor and acceptor *i* and *j* NBO orbitals.
[c] $F(i,j)$ is the Fock matrix element between i and j NBO orbitals.

dimer structure (in DMSO), which observed at (missed C1), 134.14, 114.36, 162.38, 112.67, and 137.58 ppm, respectively. C_5 atom has smaller chemical shifts than the other ring carbon atoms, due to shielding effect which the non-electronegative property of $B(OH)_2$ group. Taking into account that the range of ^{13}C NMR chemical shift C_4 are observed and calculated greater than this range, this shift can

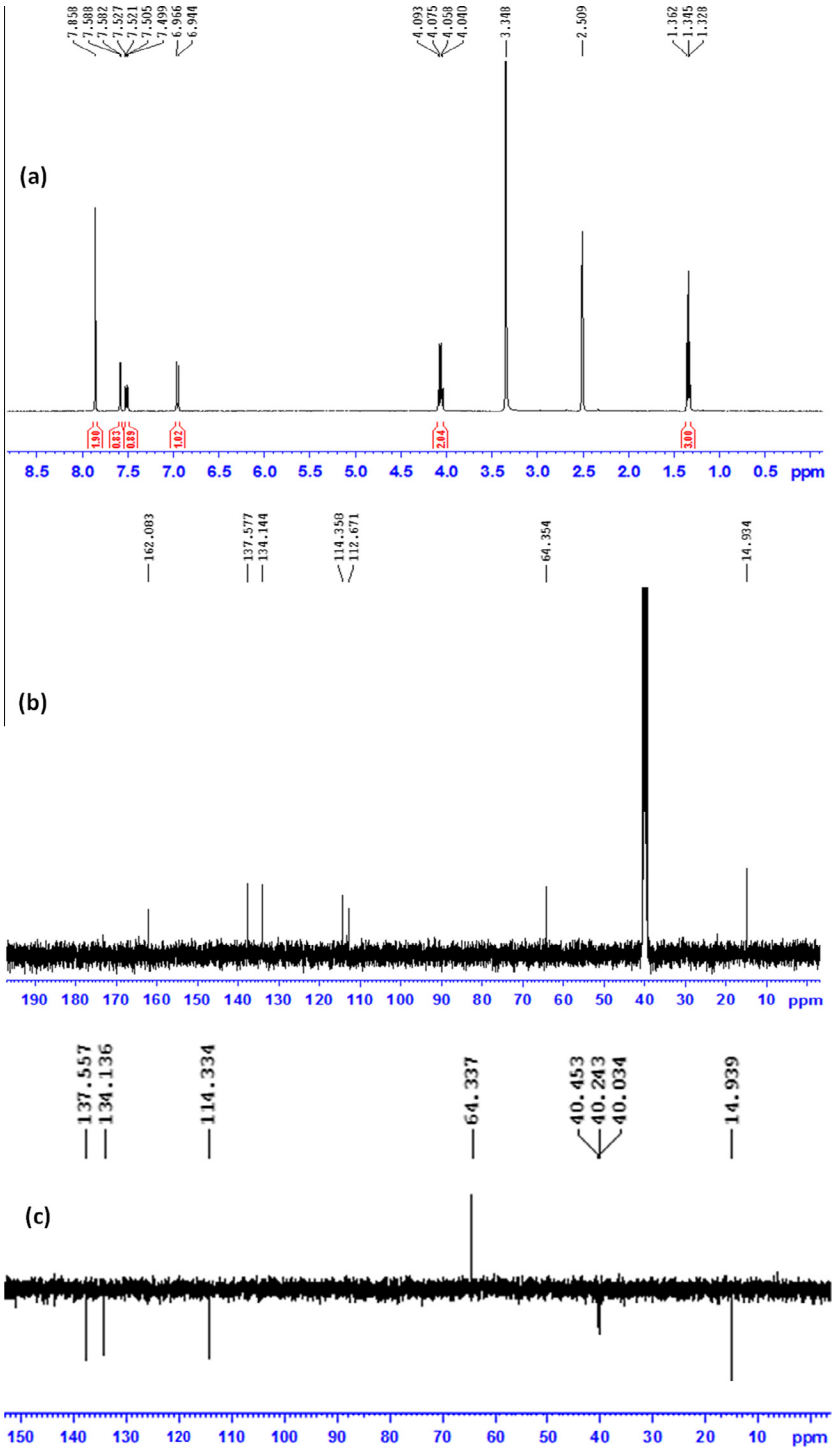

Fig. 5. (a) ^{1}H NMR (b) ^{13}C NMR (c) DEPT NMR spectra of 5Br2EPBA in DMSO.

be due to the ethoxy group attached to this carbon. The chemical shift of C_4 observed at 162.08 ppm experimentally (see Fig. 5b), while which is calculated at 166.43 by using B3LYP/6-31G(d), 169.93 ppm (monomer) and 169.87 ppm (dimer) (in DMSO) by using B3LYP/6-311G(d,p) levels, respectively. Taking a glance at the literature; the results are showed very good correlation for the structurally similar molecules [19–21,33]. The experimental value of C_1 atom is missed; this can be attached bromine atom.

The correlation graphic between the experimental and theoretical total chemical shifts of the title molecule is given in Fig. S4 for monomer and dimer structures. The correlation of dimer structure is the same for monomer structure. ^{1}H and ^{13}C NMR correlation graphics (monomer and dimer) are given Figs. S5 and S6. The relations between the calculated and experimental chemical shifts for monomer structure (δ_{exp}) are usually linear and described by the following equations {B3LYP/6-311G(d,p)}:

$$\delta_{cal}\ (\text{ppm}) = 1.0492\delta_{exp} - 0.4084 \quad (\text{Total} : R^2 = 0.9989)$$

$$\delta_{cal}\ (\text{ppm}) = 0.9554\delta_{exp} + 0.1334 \quad (^{1}\text{H} : R^2 = 0.9890)$$

Table 6
Experimental and theoretical (monomer and dimer structures), ^{1}H and ^{13}C NMR isotropic chemical shifts (with respect to TMS) of 5B2EPBA with DFT (B3LYP/6-31G(d) and 6-311G(d,p)) methods.

Atom	Experimental	6-31G(d) Monomer		6-31G(d) Dimer		6-311G(d,p) Monomer		6-311G(d,p) Dimer	
	DMSO	DMSO	Gas	DMSO	Gas	DMSO	Gas	DMSO	Gas
C1	–	134.98	137.56	117.46	120.01	134.00	136.89	134.21	137.03
C2	134.14	139.45	138.47	121.30	120.25	140.04	138.81	140.03	138.65
C3	114.36	116.73	114.39	98.84	96.46	114.59	111.64	114.72	111.70
C4	162.08	166.43	164.97	148.42	146.93	169.93	168.51	169.87	168.41
C5	112.67	125.21	125.91	107.45	108.31	124.18	124.93	124.68	125.69
C6	137.58	143.50	145.22	125.33	127.14	143.41	145.31	143.59	145.65
C15	64.35	72.65	71.91	55.16	54.38	66.00	65.09	66.21	65.31
C18	14.93	25.56	25.76	7.57	7.75	14.57	14.77	14.54	14.74
H7	7.50	7.66	7.49	6.89	6.72	7.46	7.29	7.31	7.50
H8	6.94	7.07	6.68	6.30	5.91	6.82	6.43	6.45	6.85
H9	7.59	8.07	8.25	7.36	7.56	7.87	8.03	8.12	7.93
H19	1.36	1.96	1.97	1.20	1.21	1.48	1.49	1.56	1.55
H20	1.33	1.72	1.59	0.98	0.86	1.32	1.19	1.24	1.37
H21	1.35	1.96	1.97	1.21	1.21	1.48	1.49	1.56	1.55
H16	4.06	4.46	4.29	3.74	3.58	3.95	3.78	3.83	4.00
H17	4.04	4.46	4.29	3.74	3.57	3.95	3.78	3.83	4.00
H12	–	4.35	3.95	4.81	4.84	3.86	3.43	8.46	8.42
H23	7.86	7.31	7.04	6.29	5.93	7.02	6.72	7.14	7.52

Table 7
The experimental and calculated absorption wavelength (λ, nm), excitation energies (E, eV) and oscillator strengths (*f*) of 5Br2EPBA.

Experimental		TD-DFT/B3LYP/6-311G(d,p)				CIS/B3LYP/6-311G(d,p)			
λ (nm)	*E* (eV)	λ (nm)	*E* (eV)	Major contributions (%)	*f*	λ (nm)	*E* (eV)	*f*	Major contributions (%)
Ethanol									
290.81	4.2640	**275.12**	4.5066		0.0753	**219.65**	5.6447	0.1557	
		(61 → 62)		90		(61 → 62)			81
		(60 → 63)		7		(60 → 63)			14
		244.65	5.0678		0.0001	**205.63**	6.0294	0.0173	
		(61 → 64)		98		(60 → 62)			50
						(61 → 63)			44
230.27	5.3850	**227.59**	5.4476		0.1326	**199.12**	6.2267	0.0009	
		(61 → 63)		67		(61 → 64)			75
		(60 → 62)		28		(58 → 64)			11
Water									
296.18	4.1866	**275.10**	4.5069		0.0741	**219.47**	5.6493	0.1501	
		(61 → 62)		90		(61 → 62)			90
		(60 → 63)		7		(60 → 63)			15
		244.77	5.0654		0.0001	**205.50**	6.0332	0.0174	
		(61 → 64)		98		(60 → 62)			50
						(61 → 63)			44
233.70	5.3059	**227.54**	5.4489		1.307	**199.07**	6.2281	0.0009	
		(61 → 63)		67		(61 → 64)			75
		(60 → 62)		28		(58 → 64)			11
Gas phase									
		273.42	4.5346		0.0544	**217.21**	5.7082	0.0879	
		(61 → 62)		89		(61 → 62)			76
		(60 → 63)		8		(60 → 63)			19
		241.29	5.1383		0.0001	**204.10**	6.0748	0.0202	
		(61 → 64)		98		(60 → 62)			48
						(61 → 62)			45
		212.07	5.8465		0.0003	**198.23**	6.2536	0.0007	
		(59 → 62)		99		(61 → 64)			27
						(61 → 65)			36
						(61 → 66)			11

HOMO number is 61.

$$\delta_{cal}\ (\text{ppm}) = 1.0559\delta_{exp} - 1.2502 \quad (^{13}C : R^2 = 0.9952)$$

Based on the ^{1}H and ^{13}C chemical shifts data collected in Table 6 one can deduce that qualitatively the ^{1}H and ^{13}C NMR chemical shifts of the studied molecule are described fairly well. Also the results of dimer structure are showed good correlation with their monomers.

Electronic properties

UV–Vis spectra and frontier molecular orbital analysis

The UV–Vis (electronic absorption) spectrum of 5Br2EPBA molecule is recorded in ethanol and water at room temperature. The optimized geometry in the ground state used to obtain framework of

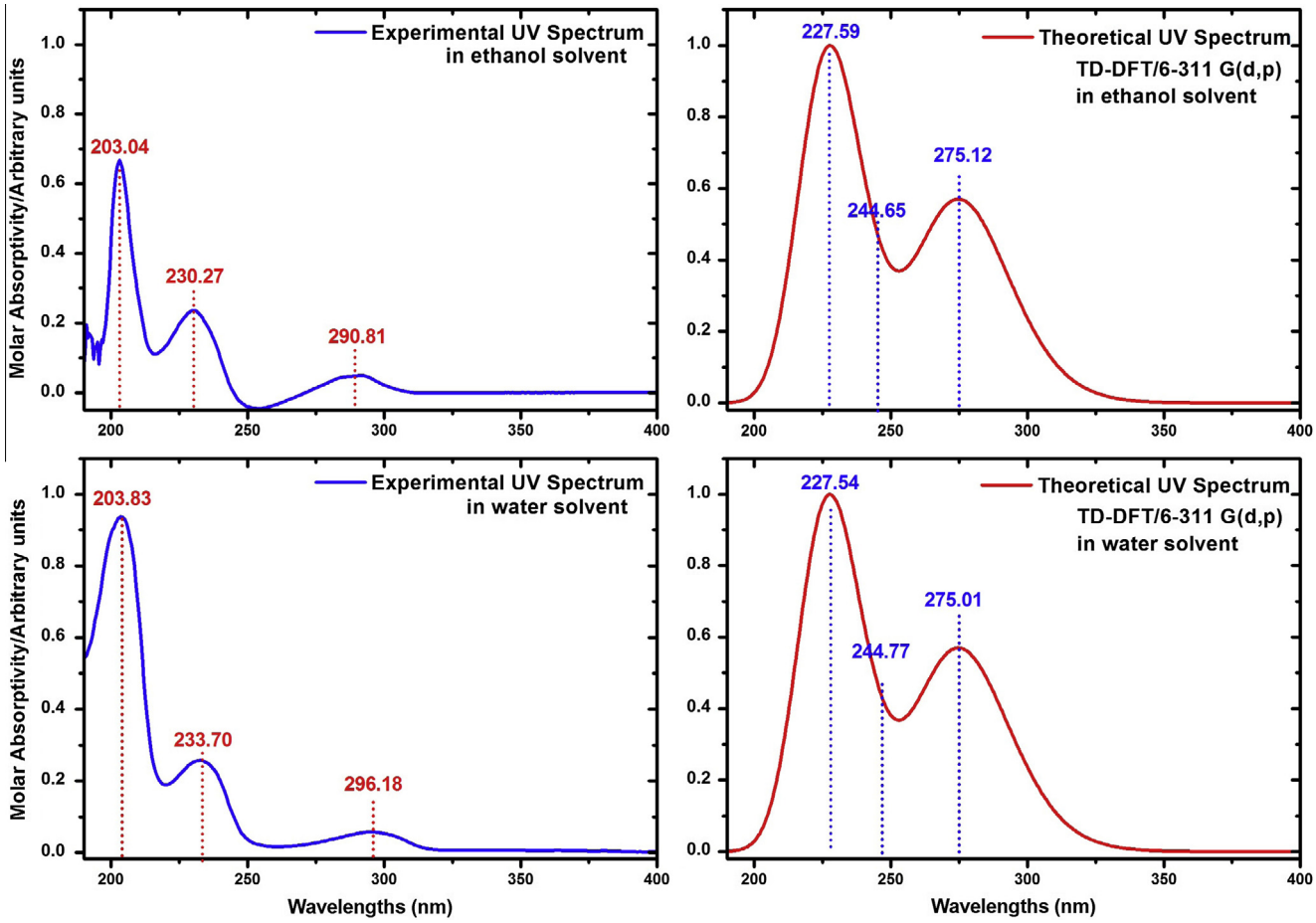

Fig. 6. The experimental and theoretical UV–Vis spectra of 5Br2EPBA in ethanol and water.

TD-DFT and CIS method with B3LYP/6-311G(d,p). TD-DFT methods are computationally more expensive than semi-empirical methods but allow easily studies of medium size molecules [49]. The electronic values, such as absorption wavelengths (λ), excitation energies (E), oscillator strengths (f), and major contributions of the transitions and assignments of electronic transitions and experimental absorption wavelengths (energies) are gathered in Table 7 for two solvents (ethanol and water). The experimental and theoretical UV–Vis spectra of the studied molecule are given in Fig. 6. The theoretical absorption bands are computed at 275.12, 244.65 and 227.59 nm for TD-DFT and at 219.65, 205.63 and 199.12 nm for CIS, in ethanol. They are also calculated at 275.10, 244.77 and 227.54 nm for TD-DFT and at 219.47, 205.50 and 199.07 nm for CIS, in water. The maximum absorption values are observed at 290.81 and 230.27 nm in ethanol and 296.18, 233.70 nm in water. TD-DFT calculations predicted the electronic absorption spectra as a quite reasonable and agreement. With CIS method at 6-311G(d,p) level, the theoretical transitions show larger deviations with the experimental results, as well as oscillator strength of more than unity, which result from the degeneracy of real electronic systems, is not surprising as the traditional with errors of 1–2 eV and more, traditional CIS and TDHF methods are considerably less accurate than TD-DFT, despite similar or higher computational requirements [50] and has almost exclusively been used for geometry optimization of excited states in larger systems, is considerably less accurate at similar or even larger computational cost [50].

The frontier molecular orbitals (FMOs) lie at the outermost boundaries of the electrons of the molecules. The most important ones called highest occupied molecular orbital (HOMO) and the lowest unoccupied molecular orbital (LUMO). HOMO and LUMO have the ability of electron giving and accepting characterizes, respectively. The physicists and chemists use their properties for the main orbital taking part in chemical reaction. These are used by the frontier electron density for predicting the most reactive position in π-electron systems and also explains several types of reaction in conjugated system [51]. The conjugated molecules are determined by a small HOMO–LUMO separation, which is the result of a significant degree of intramolecular charge transfer from the end-capping electron-donor groups to the efficient electron-acceptor group through-π conjugated path [52].

To see the bonding scheme of the studied molecule, the frontier orbitals are represented the surfaces. The energy gap is a critical parameter in determining molecular electrical transport properties because it is a measure of electron conductivity. The energy gap are calculated 5.18 eV for 5Br2EPBA molecule. The plots of FMOs ($H-2 \rightarrow L+1$, $H \rightarrow L$, and $H \rightarrow L+2$, are showed in Fig. 7. The nodes of HOMO orbitals placed on the ring, bromine atom and a bit oxygen atom of ethoxy group. But the nodes of LUMO orbitals placed symmetrically over ring and $B(OH)_2$ the molecule (except bromine atom and ethoxy group). The red color is positive and green color is the negative phase. The charge of bromine atom and $B(OH)_2$ group alternated from HOMO to LUMO of the current molecule. The FMOs, HOMO, and LUMO energy gaps explain the eventual charge transfer interactions taking place within the molecule. The FMOs energy values are calculated by B3LYP/6-311G (d,p) method for gas phase, in ethanol and water solutions: $E_{HOMO} = -6.32$, -6.41, -6.42 eV and $E_{LUMO} = -1.14$, -1.24, -1.25 eV and Energy $gap_{HOMO-LUMO} = 5.18$, 5.17, 5.17 eV. The energy gap_{H-L} and other energy gaps ($H-1 \rightarrow L$, $H \rightarrow L$, $H \rightarrow L+1$, $H \rightarrow L+2$, $H-1 \rightarrow L+2$, and $H-2 \rightarrow L+1$ are

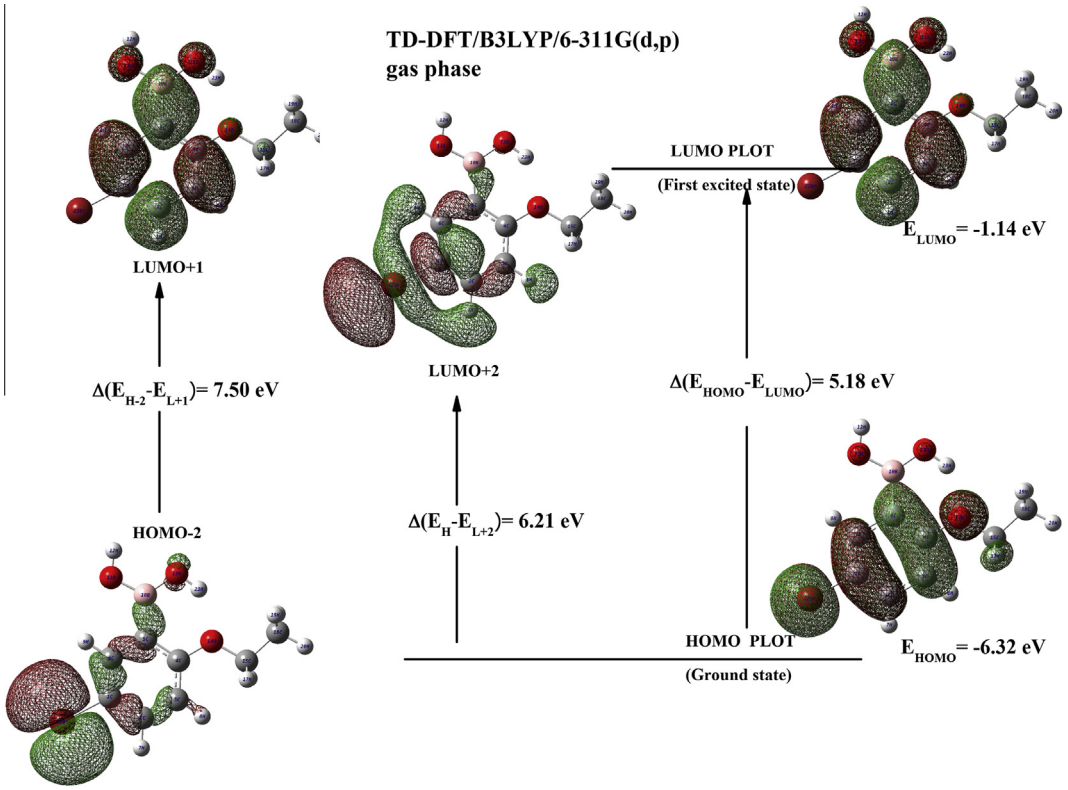

Fig. 7. The selected frontier molecular orbitals of 5Br2EPBA with the energy gaps.

Table 8
Calculated energies values of 5Br2EPBA molecule using by the TD-DFT and CIS -B3LYP method using 6-311G(d,p) basis set for TC conformer.

	TD-DFT/B3LYP/6-311G(d,p)			CIS/B3LYP/6-311G(d,p)		
	Gas	Ethanol	Water	Gas	Ethanol	Water
E_{total} (Hartree)	−3135.8184290	−3135.8270168	−3135.8274163	−3132.5931526	−3130.6810095	−3130.6814627
E_{HOMO} (eV)	−6.32	−6.41	−6.42	−8.69	−8.80	−8.80
E_{LUMO} (eV)	−1.14	−1.24	−1.25	2.50	2.42	2.41
E_{HOMO-1} (eV)	−7.35	−7.46	−7.46	−9.68	−9.77	−9.78
E_{HOMO-2} (eV)	−7.82	−8.11	−8.13	−11.17	−11.48	−11.49
E_{LUMO+1} (eV)	−0.32	−0.41	−0.42	3.54	3.45	3.44
E_{LUMO+2} (eV)	−0.11	−0.29	−0.3	3.77	3.80	3.79
$E_{HOMO-1-LUMO\ gap}$ (eV)	**6.21**	**6.22**	**6.21**	**12.18**	**12.19**	**12.19**
$E_{HOMO-LUMO\ gap}$ (eV)	**5.18**	**5.17**	**5.17**	**11.19**	**11.22**	**11.21**
$E_{HOMO-LUMO+2\ gap}$ (eV)	**6.21**	**6.12**	**6.12**	**12.46**	**12.60**	**12.59**
$E_{HOMO-1-LUMO+2\ gap}$ (eV)	**7.24**	**7.17**	**7.16**	**13.45**	**13.57**	**13.57**
$E_{HOMO-2-LUMO+1\ gap}$ (eV)	**7.50**	**7.70**	**7.71**	**14.71**	**14.93**	**14.93**
Chemical hardness (h)	2.59	2.59	2.59	5.60	5.61	5.61
Electronegativity (χ)	3.73	3.83	3.84	3.10	3.19	3.20
Chemical potential (μ)	−3.73	−3.83	−3.84	−3.10	−3.19	−3.20
Electrophilicity index (ω)	2.69	2.83	2.84	0.86	0.91	0.91

calculated 6.21, 5.18, 6.21, 7.24, and 7.50 eV, respectively for gas phase TD−DFT/B3LYP/6-311G(d,p) (see Table 8). These values are calculated in two solvents of the title molecule. CIS/B3LYP/6-311G(d,p) method are also utilized to comparison. The value of chemical hardness is 2.59 eV in gas phase, ethanol and water. The Electrophilicity index (ω) and electronegativity (χ) are increasing 0.1 eV in solvents. All values are collected in Table 8 both TD-DFT and CIS method.

Total, partial, and overlap population density-of-states

The neighboring orbitals may show quasi degenerate energy levels in the boundary region. To obtain a pictorial representation of MO (molecule orbital) compositions and their contributions to chemical bonding, the density of state of the title molecule (TDOS, PDOS and OPDOS) are given in Figs. 8–10, respectively. The TDOS, PDOS, and OPDOS or COOP (Crystal Orbital Overlap Population) density of states [53,54] are obtained by convoluting the molecular orbital information with Gaussian curves of unit height and Full width at half maximum (FWHM) of 0.3 eV, using the GaussSum 2.2 program [32]. The OPDOS graphs show bonding, anti-bonding and nonbonding nature of the interaction of the two orbitals in atoms or groups. The negative and positive values indicate a bonding interaction and an anti-bonding interaction and zero value indicates nonbonding interactions, respectively [55]. Moreover they allow us to the determination and comparison of the donor–acceptor properties of the ligands and ascertain the bonding, non-bonding.

The PDOS mainly presents the composition of the fragment orbitals contributing to the molecular orbitals. The HOMO orbitals are localized on the ring (C_6H_3 group), ethoxy (CH_3CH_2O– group) and Bromine atom (62% + 15% + 22% = 99%) and $B(OH)_2$ group (a bit O atoms) (1%), while LUMO orbitals spread on the ring (C_6H_3 group) and $B(OH)_2$ group (83% + 16% = 99%) and group (a bit C and O atoms in ethoxy group) (1%). However to have information about bonding and anti-bonding properties is very hard according to percentage sharing of atomic orbitals or molecular fragments in the molecule. Therefore the OPDOS diagram (some of its orbitals of energy values of interaction between selected groups) is shown on the figure easily, ring ↔ $B(OH)_2$ group (black line) system is positive (bonding interaction) also ring ↔ bromine atom (green line) system is negative (anti-bonding), and also ring ↔ ethoxy group (pink line) system is negative (anti-bonding). The other line (red, blue, and navy blue) system is nearly zero (non-bonding). As can be seen from the OPDOS plots for studied molecule have anti-bonding (negative range) character in frontier HOMO and LUMO molecular orbital (except for HOMO of ring group and bromine atom).

Molecular electrostatic potential surface

The importance of MEP lies in the fact that it simultaneously displays molecular size, shape as well as positive, negative and neutral electrostatic potential regions in terms of color grading (Fig. 11) and is very useful in research of molecular structure with its physiochemical property relationship [56,57]. They generally showed that the maximum positive region which preferred site for nucleophilic attack symptoms as blue color, while the maximum negative region which preferred site for electrophilic attack indications as red color.

The MEPs of 5Br2EPBA molecule is plotted as 3D and 2D contour map plots in Fig. 11. The electrostatic potential values are showed by different colors for different data in the map of MEPs. The potential values increase from red to blue color. The colors are range between −0.04411 a.u. (dark red) and 0.04411 a.u. (dark blue) for the title molecule. The red and blue colors show strongest repulsion and attraction, respectively. The MEPs map of 5Br2EPBA indicated that while regions having the positive potential are near H atom ($B(OH)_2$ and ethoxy groups), the regions having the negative potential are over the oxygen atoms and bromine atom. From these results, we can say that near the H atoms (especially H_{12}) indicate the strongest attraction while O atoms the strongest repulsion (see Fig. 11).

The map of sliced 2D MEPs contour provides more exhaustive information regarding molecular electrostatic potential distribution, by showing the values in an assortment of spatial site around the molecule. The 2D MEPs are pictured in the molecular plane of the title molecule. The around of the oxygen atoms and bromine atom have been electron rich region and all the around of hydrogen atoms correspond to the electron deficient region. The negative and positive values (as a maximum) potential corresponding to the nucleophilic and electrophilic region are −0.02 a.u. (near the O atoms and Br atom) and 0.2 a.u. (center of molecule), respectively.

Mulliken atomic charges

The Mulliken atomic charges are calculated by determining the electron population of each atom as defined by using the DFT/B3LYP method 6-311G(d,p) basis set for monomer and dimer structures of TC conformer. The atomic charges display an important role in the application of quantum mechanical calculations the molecular system. The Mulliken atomic charges of the title molecule (for monomer and dimer structures) were gathered in Table 9 and given in Fig. S7. The Mulliken charges of phenyl boronic acid were done previously and compared the other derivatives of phenyl boronic acid [19,20]. In this paper, the charges of phenyl boronic acid are not given again and we took care prior studies [19,20] for phenylboronic acid. The bromine atom and ethoxy

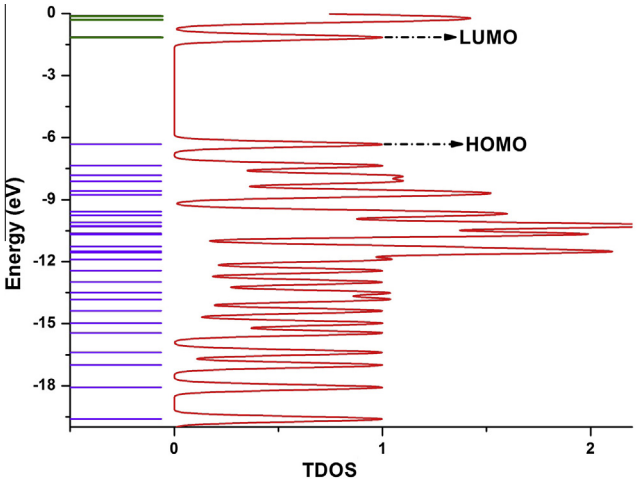

Fig. 8. The TDOS diagram of 5Br2EPBA.

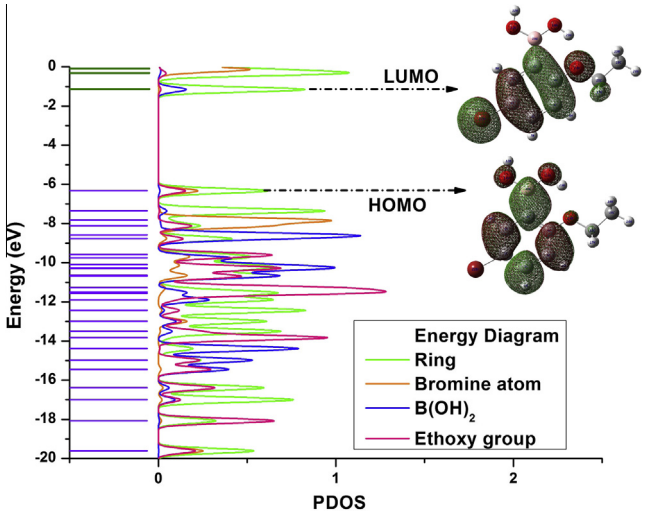

Fig. 9. The PDOS diagram of 5Br2EPBA.

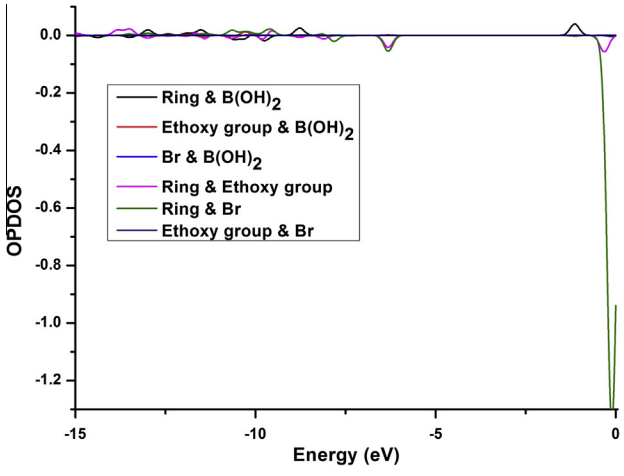

Fig. 10. The OPDOS diagram of 5Br2EPBA.

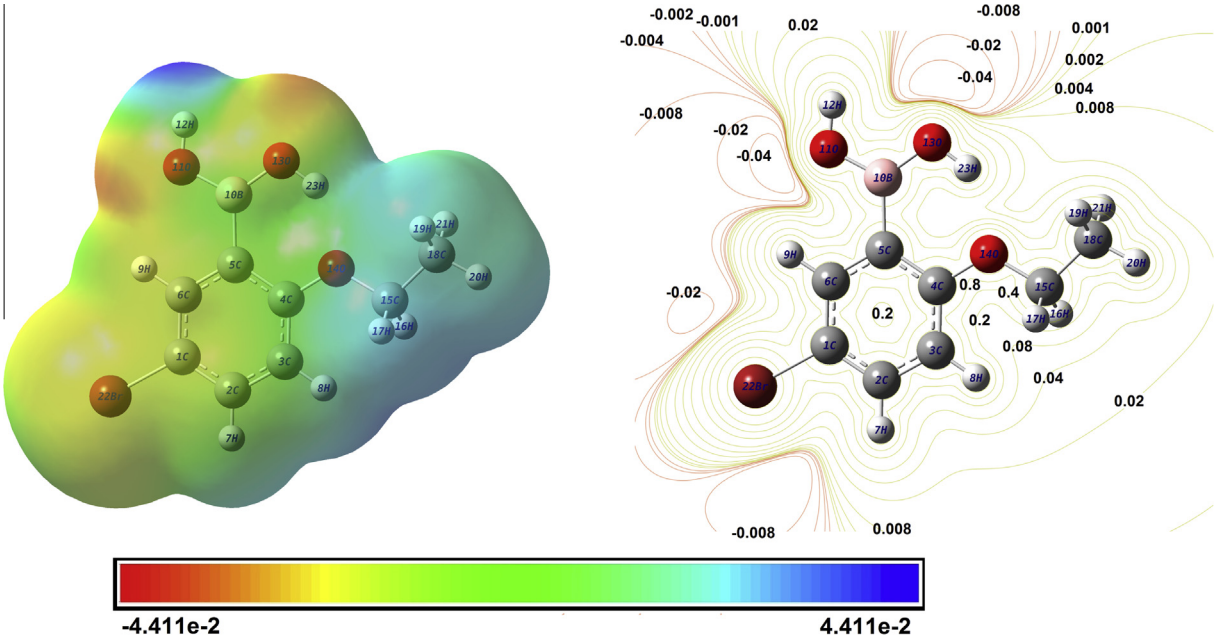

Fig. 11. The MEPs 3D map and 2D contour map for 5Br2EPBA molecule.

group (substitution of phenylboronic acid) lead to redistribution of electron density. The charge distribution of $B(OH)_2$ group showed the same charge (negative or positive) with the phenylboronic acid [19,20], however, the charges of aromatic ring of the title molecule show different charge with each other. For example, charge of C_6 atom is positive in phenyl boronic acid [19,20], however, the value of Mulliken atomic charge of this atom is negative in our molecule. Hydrogen atoms exhibit a positive charge, which is an acceptor atoms both each molecules [19,20]. The Mulliken atomic charges of monomer and dimer structures of the title molecule are seen as similar distributions. However the bromine atom replaced the H showed as a negative charge.

Thermodynamic features

The thermodynamical parameters such as: zero-point vibrational energy, rotational constants, thermal energy, specific heat capacity, entropy and dipole moment of TC form of the current molecule are calculated and listed in Table S3 at room temperature (298.15 K) in the ground state by using DFT/B3LYP/6-311G(d,p) method both C_1 and C_s symmetry point group.

The heat capacity (C), entropy (S) and enthalpy changes (ΔH) are reported to view depending on the temperature change of the thermodynamic functions increasing the temperature gradually varied every 50 K, from 100 to 700 K. The statically thermodynamic functions (C, S and ΔH) of the present molecule are obtained from the theoretical harmonic frequencies and given in Table S4. The thermodynamic functions are rising with temperature, due to the fact that the molecular vibrational intensities increase with temperature. Correlation graphics of these are represented in Fig. S8. The correlation equations between heat capacity, entropy, enthalpy changes and temperatures are fitted by quadratic formulas and the corresponding fitting factors (R^2) for these thermodynamic properties are 0.9997, 0.9999 and 0.9999, respectively. The corresponding fitting equations:

$$C = 4.41110 + 0.17015T - 7.4414 \times 10^{-5}T^2 \quad (R^2 = 0.9997)$$

$$S = 59.2837 + 0.21115T - 6.4824 \times 10^{-5}T^2 \quad (R^2 = 0.9999)$$

Table 9
Comparison of Mulliken charges of 5Br2EPBA by using B3LYP/6-311G(d,p) basis set for monomer and dimer structures of TC conformer.

Atoms	Monomer	Dimer
C1/24	−0.184	−0.183
C2/25	−0.015	−0.016
C3/26	−0.119	−0.116
C4/27	0.198	0.199
C5/28	−0.190	−0.192
C6/39	−0.040	−0.039
H7/30	0.112	0.111
H8/31	0.110	0.111
H9/32	0.122	0.121
B10/33	0.393	0.440
O11/34	−0.349	−0.365
H12/35	0.249	0.276
O13/36	−0.347	−0.418
O14/37	−0.424	−0.433
C15/38	−0.036	−0.034
H16/39	0.119	0.119
H17/40	0.119	0.119
C18/41	−0.307	−0.309
H19/42	0.124	0.125
H20/43	0.116	0.117
H21/44	0.124	0.125
Br22/45	−0.037	−0.038
H23/46	0.263	0.280

$$\Delta H = -0.84383 + 0.01614T + 5.6150 \times 10^{-5}T^2 \quad (R^2 = 0.9999)$$

These data help to have information for the further study on 5Br2EPBA. To calculate the other thermodynamic energies according to relationships of thermodynamic functions and estimate directions of chemical reactions according to the second law of thermodynamics in thermochemical field, the results of thermodynamic calculations can be used.

Nonlinear optical properties

The investigation of electronic dipole moment, polarizability, anisotropy of polarizability and first hyperpolarizability for the title molecule are presented in this part. To have polarizability and hyperpolarizability tensors (α_{xx}, α_{xy}, α_{yy}, α_{xz}, α_{yz}, α_{zz} and β_{xxx},

β_{xxy}, β_{xyy}, β_{yyy}, β_{xxz}, β_{xyz}, β_{yyz}, β_{xzz}, β_{yzz}, β_{zzz}) are utilized a frequency job output file of Gaussian. However, the units of α and β values of Gaussian output are in atomic units (a.u.) therefore they have been converted into electronic units (esu) (for α; 1 a.u. = 0.1482×10^{-24} esu, for β; 1 a.u. = 8.6393×10^{-33} esu). The mean polarizability (α), anisotropy of polarizability ($\Delta\alpha$) and the average value of the first hyperpolarizability $\langle\beta\rangle$ can be calculated using the equations.

$$\alpha_{tot} = \frac{1}{3}(\alpha_{xx} + \alpha_{yy} + \alpha_{zz})$$

$$\Delta\alpha = \frac{1}{\sqrt{2}}\left[(\alpha_{xx} - \alpha_{yy})^2 + (\alpha_{yy} - \alpha_{zz})^2 + (\alpha_{zz} - \alpha_{xx})^2 + 6\alpha_{xz}^2 + 6\alpha_{xy}^2 + 6\alpha_{yz}^2\right]^{\frac{1}{2}}$$

$$\langle\beta\rangle = \left[(\beta_{xxx} + \beta_{xyy} + \beta_{xzz})^2 + (\beta_{yyy} + \beta_{yzz} + \beta_{yxx})^2 + (\beta_{zzz} + \beta_{zxx} + \beta_{zyy})^2\right]^{\frac{1}{2}}$$

These parameters are gathered and listed in Table S5, described above and electronic dipole moment and total {μ_i ($i = x,y,z$) and μ_{tot}} for 5Br2EPBA molecule. The total dipole moment can be calculated using the following equation.

$$\mu_{tot} = \left(\mu_x^2 + \mu_y^2 + \mu_z^2\right)^{\frac{1}{2}}$$

It is well known that the higher values of dipole moment, molecular polarizability, and hyperpolarizability are important for more active NLO properties. The title molecule has relatively homogeneous charge distribution and it does not have large dipole moment. The calculated value of the dipole moment is found to be 4.5102 Debye. The highest value of the dipole moment is observed for component μ_x. In this direction, this value is equal to −4.5088 Debye and μ_z is the smallest one as zero. The calculated polarizability and anisotropy of the polarizability of the title molecule is $19.090534 \times 10^{-24}$ esu and $50.05554725 \times 10^{-24}$ esu, respectively. The magnitude of the molecular hyperpolarizability β, is one of important key factors in a NLO system. The first hyperpolarizability value (β) of 5Br2EPBA is equal to $1395.674892 \times 10^{-33}$ esu, by using B3LYP/6-311G(d,p) method. Based on NLO properties of (common values) urea; the first hyperpolarizability, polarizability and anisotropy of the polarizability values of 5Br2EPBA are bigger than those of urea.

Conclusions

The spectroscopic features of derivative of phenyl boronic acid is investigated by combined FT-IR, FT-Raman UV–Vis, ^{1}H, ^{13}C and DEPT NMR spectroscopies and quantum chemical calculations to identify vibrational assignments, magnetic and electronic properties of 5Br2EPBA molecule. The optimized geometric parameters (bond lengths and bond angles) are theoretically determined and compared with the structurally similar molecules. The hydrogen bonded interaction between two monomeric units of 5Br2EPBA molecule and consequently the counterpoise corrected interaction energy has also been calculated. Further the short (O–H···O) of the hydrogen bonds (ca. 1.817 Å) indicates strong hydrogen bonding between the monomeric units. FT-IR and FT-Raman spectra of the title molecule are observed with experimental and calculated (monomer and dimer structures) vibrational wavenumbers. The assignments of wavenumbers are made with TED. The magnetic properties of 5Br2EPBA molecule are carried out from ^{1}H, ^{13}C and DEPT NMR spectra in DMSO and calculated (monomer and dimer structures) by GIAO method. The energies of the important molecular orbitals and the electronic absorption wavelengths of the studied molecule are also investigated by TD-DFT method along with the other electronic and NLO properties. The molecular orbitals and MEPs contour/surface drawn showed that the negative potential sites are on bromine and oxygen atoms as well as the positive potential sites are around the hydrogen (especially H_{12}) atoms. The thermodynamic features are obtained from DFT/B3LYP. The thermodynamic functions; heat capacity (C) entropy (S) and enthalpy changes (H) increase with the increasing temperature (100–700 K) owing to the intensities of the molecular vibrations increase with increasing temperature.

Appendix A. Supplementary material

Supplementary data associated with this article can be found, in the online version, at http://dx.doi.org/10.1016/j.saa.2014.08.049.

References

[1] W. Yang, X. Gao, B. Wang, Med. Res. Rev. 23 (2003) 346–368.
[2] X. Chen, G. Liang, D. Whitmire, J.P. Bowen, J. Phys. Org. Chem. 11 (1998) 378–386.
[3] A.M. Irving, C.M. Vogels, L.G. Nikolcheva, J.P. Edwards, X.F. He, M.G. Hamilton, M.O. Baerlocher, F.J. Baerlocher, A. Decken, S.A. Westcott, New J. Chem. 27 (2003) 1419–1424.
[4] E.P. Ingenito, A. Schwarz, L.W. Tsai, Polymer Systems for Lung Volume Reduction Therapy, Application number PCT/US07/79504, filed Sep. 26, 2007.
[5] D.G. Hall, Boronic Acids, Wiley-VCH Verlag GmbH &Co. KGaA, Weinheim, 2005.
[6] M.R. O'Donovan, C.D. Mee, S. Fenner, A. Teasdale, D.H. Phillips, Mutat. Res. 724 (2011) 1–6.
[7] J.N. Cambre, B.S. Sumerlin, Polymer (Guildf) 52 (2011) 4631–4643.
[8] P.R. Westmark, B.D. Smith, J. Pharm. Sci. 85 (1996) 266–269.
[9] S. Rettig, J. Trotter, Can. J. Chem. 55 (1977) 3071–3075.
[10] M.K. Cyrański, A. Jezierska, P. Klimentowska, J.J. Panek, A. Sporzyński, J. Phys. Org. Chem. 21 (2008) 472–482.
[11] P. Rodríguez-Cuamatzi, H. Tlahuext, H. Höpfl, Acta Crystallogr. Sect. E 65 (2008) o44–o45.
[12] M.R. Shimpi, N. Seetha Lekshmi, V.R. Pedireddi, Cryst. Growth Des. 7 (2007) 1958–1963.
[13] J.A. Faniran, H.F. Shurvell, Can. J. Chem. 46 (1968) 2089–2095.
[14] M. Kurt, J. Raman Spectrosc. 40 (2009) 67–75.
[15] M. Karabacak, E. Kose, A. Atac, E.B. Sas, A.M. Asiri, M. Kurt, J. Mol. Struct. 1076 (2014) 358–372.
[16] M. Kurt, T. Raci Sertbakan, M. Özduran, M. Karabacak, J. Mol. Struct. 921 (2009) 178–187.
[17] S. Ayyappan, N. Sundaraganesan, M. Kurt, T.R. Sertbakan, M. Özduran, J. Raman Spectrosc. 41 (2010) 1379–1387.
[18] Ö. Alver, C. Parlak, Vib. Spectrosc. 54 (2010) 1–9.
[19] M. Karabacak, E. Kose, A. Atac, M.A. Cipiloglu, M. Kurt, Spectrochim. Acta A 97 (2012) 892–908.
[20] M. Karabacak, E. Kose, A. Atac, A.M. Asiri, M. Kurt, J. Mol. Struct. 1058 (2014) 79–96.
[21] M. Karabacak, L. Sinha, O. Prasad, A.M. Asiri, M. Cinar, Spectrochim. Acta Part A Mol. Biomol. Spectrosc. 115 (2013) 753–766.
[22] U. Rani, M. Karabacak, O. Tanrıverdi, M. Kurt, N. Sundaraganesan, Spectrochim. Acta A 92 (2012) 67–77.
[23] A.K. Sachan, S.K. Pathak, L. Sinha, O. Prasad, M. Karabacak, A.M. Asiri, J. Mol. Struct. 1076 (2014) 639–650.
[24] M. Frisch, et al., Wallingford, CT, 2009.
[25] P. Hohenberg, W. Kohn, Phys. Rev. 136 (1964) B864–B871.
[26] A.D. Becke, J. Chem. Phys. 98 (1993) 5648–5652.
[27] C. Lee, W. Yang, R.G. Parr, Phys. Rev. B 37 (1988) 785–789.
[28] J. Baker, A.A. Jarzecki, P. Pulay, J. Phys. Chem. A 102 (1998) 1412–1424.
[29] J. Baker, K. Wolinski, Parallel Quantum Solut. 2013 Green Acres Road, Suite A, Fayetteville, AR 72703.
[30] R. Ditchfield, J. Chem. Phys. 56 (1972) 5688–5691.
[31] K. Wolinski, J.F. Hinton, P. Pulay, J. Am. Chem. Soc. 112 (1990) 8251–8260.
[32] N.M.O. Boyle, A.L. Tenderholt, K.M. Langner, J. Comput. Chem. 29 (2008) 839–845.
[33] Y. Erdogdu, M. Tahir Gulluoglu, M. Kurt, J. Raman Spectrosc. 40 (2009) 1615–1623.
[34] K.L. Bhat, N.J. Howard, H. Rostami, J.H. Lai, C.W. Bock, J. Mol. Struct. Theochem. 723 (2005) 147–157.
[35] Z. Liu, Y. Qu, M. Tan, H. Zhu, Acta Crystallogr. Sect. E60 (2004) o1310–o1311.
[36] M. Karabacak, M. Kurt, J. Mol. Struct. 919 (2009) 215–222.
[37] M. Karabacak, M. Cinar, A. Coruh, M. Kurt, J. Mol. Struct. 919 (2009) 26–33.
[38] Y.M. Wu, C.C. Dong, S. Liu, H.J. Zhu, Y.Z. Wu, Acta Crystallogr. Sect. E 62 (2006) o4236–o4237.
[39] R.M. Silverstein, F.X. Webster, D.J. Kiemle, Spectrometric Identification of Organic Compounds, John Wiley & Sons, 2005.
[40] G. Kahraman, O. Beşkardeş, Z.M.O. Rzaev, E. Pişkin, Polymer (Guildf) 45 (2004) 5813–5828.
[41] G. Varsányi, Assignments for Vibrational Spectra of Seven Hundred Benzene Derivatives, Halsted Press, 1974.

[42] M. Karabacak, A. Coruh, M. Kurt, J. Mol. Struct. 892 (2008) 125–131.
[43] M. Szafran, A. Komasa, E. Bartoszak-Adamska, J. Mol. Struct. 827 (2007) 101–107.
[44] J. Liu, Z. Chen, S. Yuan, J. Zhejiang Univ. Sci. B 6B (2005) 584–589.
[45] C. James, A.A. Raj, R. Reghunathan, V.S. Jayakumar, I.H. Joe, J. Raman Spectrosc. 37 (2006) 1381–1392.
[46] N. Subramanian, N. Sundaraganesan, J. Jayabharathi, Spectrochim. Acta A 76 (2010) 259–269.
[47] K. Pihlaja, E. Kleinpeter, Carbon-13 NMR Chemical Shifts in Structural and Stereochemical Analysis, VCH, 1994.
[48] H.O. Kalinowski, S. Berger, S. Braun, Carbon-13 NMR Spectroscopy, Wiley, New York, 1988.
[49] J. Fabian, Dye. Pigment 84 (2010) 36–53.
[50] F. Furche, D. Rappoport, Chapter III Comput. Photochem., in: M. Olivucci (Ed.), Theor. Comput. Chem., vol. 16, Elsevier, Amsterdam, 2005.
[51] K. Fukui, T. Yonezawa, H. Shingu, J. Chem. Phys. 20 (1952) 722.
[52] C.H. Choi, M. Kertesz, J. Phys. Chem. A 101 (1997) 3823–3831.
[53] J.G. Małecki, Polyhedron 29 (2010) 1973–1979.
[54] R. Hoffman, Solids and Surfaces: A Chemist's View of Bonding in Extended Structures, VCH Publishers, New York, 1988.
[55] M. Chen, U.V. Waghmare, C.M. Friend, E. Kaxiras, J. Chem. Phys. 109 (1998) 6854–6860.
[56] J. Murray, K. Sen, Molecular Electrostatic Potentials: Concepts and Applications, Elsevier, Amsterdam, 1996.
[57] E. Scrocco, J. Tomasi, Advances in Quantum Chemistry, vol. 11, Elsevier, 1978.